STUDIES ON PHYSICO-CHEMICAL PROPERTIES OF SYNTHETIC ZEOLITES

A THESIS SUBMITTED TO THE UNIVERSITY OF PUNE

FOR

THE DEGREE OF MASTER OF SCIENCE IN CHEMISTRY

(Partly by papers and partly by research)

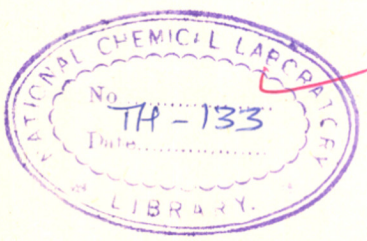

BY

V. P. SHIRALKAR
B.Sc.(Hons.)

NATIONAL CHEMICAL LABORATORY
PUNE-8
INDIA

1976

A C K N O W L E D G E M E N T

It gives me immense pleasure to record my deep sense of gratitude to Dr.(Miss) S.B. Kulkarni, for her meticulous planning and inspiring guidance throughout this investigation and also for the painstaking efforts in the preparation of the manuscript.

I am thankful to my colleagues and friends for their whole-hearted cooperation especially for recording IR, X-ray and thermograms of the zeolite samples.

Finally, I am grateful to the Director, National Chemical Laboratory, Poona-8, for allowing me to submit this investigation in the form of a thesis.

POONA
30th Aug. '76

(V. P. SHIRALKAR)

C O N T E N T S

CHAPTER – III (continued)

CHAPTER - I : INTRODUCTION

GENERAL INTRODUCTION

During the past decade, the use of crystalline zeolites has increased considerably. They are industrially used as (i) catalysts for petroleum crackings, (ii) adsorbents for selective separation of n-paraffins to upgrade certain petroleum fractions and (iii) dehydrants for exhaustive drying of gases and liquids. For continued and economical industrial applications, the zeolites should possess high thermal stability so that they can be regenerated and reused over a large number of cycles. In this thesis, physico-chemical properties and thermal stability of a series of rareearth exchanged X and Y types zeolites has been examined by thermogravimetric, X-ray, infrared and sorption measurements.

In the following is given a brief literature review on the classification and structures of zeolites. Their thermal, sorption and catalytic properties for various catalytic reactions are also indicated.

CRYSTALLINE ZEOLITES :

Zeolites are crystalline, hydrated aluminosilicates of group I and II elements. They occur in nature as well as can be synthesized. Commercially they are known as "Molecular Sieves" (Linde Company, USA) or "Microtraps" (Davison Company).

Structurally zeolites are frame-work aluminosilicates, which are based on an infinite three dimensional network of AlO_4 and SiO_4 tetrahedra. These tetrahedra are linked together by sharing oxygen ions and form a stable strongly bonded structure. The unique structural feature of molecular sieve zeolite is a narrow uniform continuous channel system that becomes available after zeolitic water has been driven off by heating and evacuation. Great thermal stability after dehydration has been observed in the structure of X and Y type faujasites.

The zeolites are represented by a general formula

$$M_{2/n}\,O : Al_2O_3 : x\,SiO_2 : y\,H_2O$$

where x is greater than or equal to 2, n is cation valency. The cations are quite mobile and can be exchanged by other cations. Intra-crystalline zeolitic water in many zeolites is removed reversibly. However, in some cases, the cation exchange or dehydration may produce structural changes in the framework.

In some of the synthetic zeolites, the aluminium cations are substituted by gallium; and silicon ions by germanium and phosphorous ions. The latter necessitates the modification of the structural formula.

The unit cell of zeolite consisting of silica alumina tetrahedra is preferably expressed by the formula :

$$M_{x/n}\left[(AlO_2)_x\,(SiO_2)_y\right] wH_2O$$

The sum (x+y) is the total number of tetrahedra in the unit cell. The parenthesis represents the framework composition. For a zeolite to be used as a molecular sieve, its structure, after complete dehydration must remain intact.

CLASSIFICATION :

In the earlier morphological classification the crystalline aluminosilicates were divided into three groups : (1) The fibrous zeolites characterized by chains of linked tetrahedra in which there is a strong binding, (2) The platty or lamellar zeolites built up of sheets linked together with weak bindings and (3) The three dimensional framework zeolites characterised by a cubic or rhombohedral structure. The last category includes the most of the well-known molecular sieve zeolites.

Due to powerfull analytical tools such as X-ray diffraction, 30 to 40 zeolite species are well defined. The newer classification is based on X-ray, the classification groups being natrolite, chabazite, heulandite, harmotone, mordenite and faujasites. The Table-1 lists the properties of some important zeolites by group.

TABLE-1 : PROPERTIES OF SOME IMPORTANT ZEOLITES OF GENERAL FORMULA

$$M_{x/n}\left[(AlO_2)_x(SiO_2)_y\right] a\ H_2O$$

Name	General formula				Symmetry	Void volume cc./gm.	Aperture size Å
	M	x	y	a			
Analcime Group							
Analcime	Na	16	32	16	Cubic	0.099	2.8
Faujasite Group							
Zeolite A	Na	12	12	27	Cubic	0.30	4.2
Faujasite	Na,Ca,Mg	60	132	260	Cubic	0.35	8.0
Zeolite X	Na	86	106	264	Cubic	0.36	8.0
Zeolite Y	Na	56	136	264	Cubic	0.35	8.0
Chabazite Group							
Chabazite	Ca	8	16	26	Rhombohedral	0.29	3.0 x 4.3
Erionite	Ca,Mg,Na	9	27	27	Hexagonal	0.21	3.6 x 5.2
Harmotone Group							
Philipsite	K,Na	5	11	10	Orthorhombic	0.22	4.0

continued.....

TABLE-1 (CONTINUED)

Name	General formula				Symmetry	Void volume cc./gm.	Aperture size $\overset{o}{A}$
	M	x	y	a			
Mordenite Group							
Mordenite	Na	8	40	24	Orthorhombic	0.14	5.8 x 7.0
Heulandite Group							
Stilbite	Na, K, Ca	10	26	28	Monoclinic	0.22	~ 2.6
Natrolite Group							
Natrolite	Na	16	24	16	-	-	-

Meier[1] has described in detail the structural framework of faujasites and many other zeolites and presented a stereogram[2]. The classification and structure of these zeolites are also reported by Barrer[3], Berghoff[4] and Turkevich[5]. An uptodate information on classification, structure, chemical composition and properties of different zeolites has been compiled by Breek[6].

UNIT CELL COMPOSITION AND CATION SITES IN TYPES X AND Y ZEOLITES :

The synthetic zeolites, X and Y types are isostructural with the rare mineral faujasite. Typical unit cell compositions of X type and Y type zeolites are represented by

$$Na_{86}(AlO_2)_{86}\ (SiO_2)_{106} \cdot 264\ H_2O$$

and

$$Na_{56}(AlO_2)_{56}(SiO_2)_{136} \cdot 250\ H_2O$$

respectively. The number of aluminium atoms in the zeolite is determined from the relation

$$N_{Al} = \frac{192}{1 + R}$$

where $R = N_{Si} / N_{Al}$. The number of aluminium atoms (N_{Al}) in the unit cell of the zeolite X varies from 96 to 77

and in zeolite Y from 76 to 48. Number of sodium ions N_{Na} is generally equal to N_{Al}. The value of R varies from 1 to 1.5 for type X zeolite and from 1.5 to 3.0 for type Y zeolite. The unit cell constant changes with the number of aluminium atoms per unit cell.

The cations occupy different positions in the zeolite. Earlier, three types of sites were recognised. Type S_I is located in the hexagonal prisms between the sodalite units. Type S_{II} is located in the open six membered faces on the sodalite unit. Type S_{III} is located on the walls of the cavity. A major difference between type X and type Y is the non-occupancy of type S_{III} sites in the type Y zeolite. According to recent nomenclature by Smith[7], the site I is situated at the centre of the hexagonal prisms I' is on the triad axis displaced into sodalite cage and hexagonal prisms. Site II' is on the triad axis but displaced into sodalite cage from the unshared six-membered oxygen ring between sodalite cage and supercage; site II is slightly and II* is considerably displaced. Site III is displaced into supercage from bridging of four-oxygen rings. Figure-1 shows the basic sodalite unit and the position of most of these sites in the X type zeolite.

Cation sites in the various zeolites determined by the X-ray diffraction have been tabulated by Rees[8].

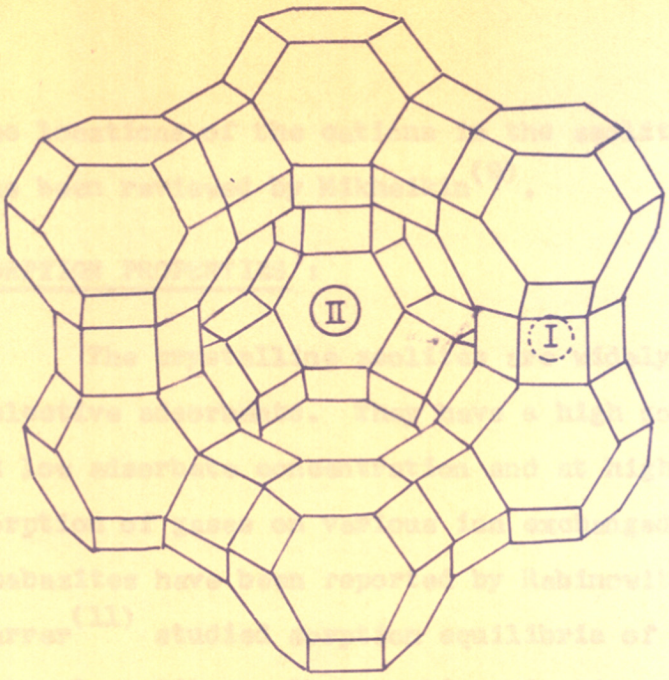

A

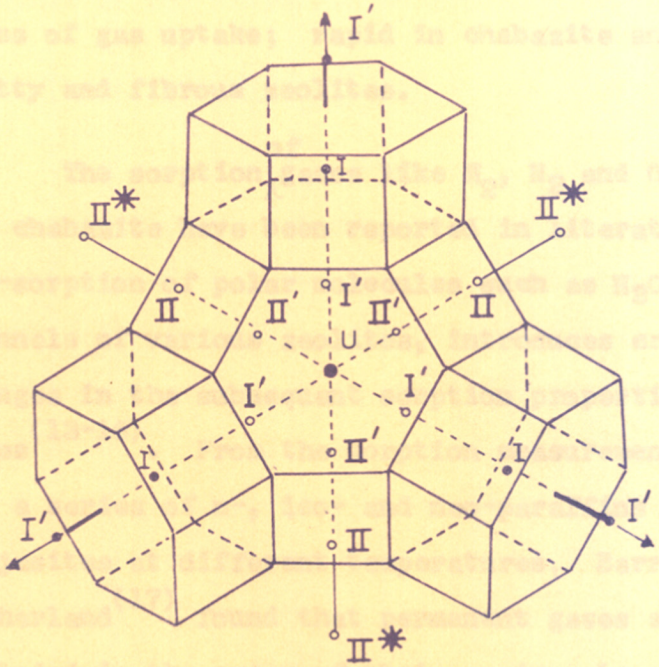

B

FIG.–1 A - PERSPECTIVE VIEW OF PART OF THE FAUJASITE STRUCTURE. I AND II ARE THE CATION SITES (Ref. 12)

B - IDEALIZED PROJECTION OF SODALITE UNIT WITH CATION SITES (Ref. 9)

The locations of the cations in the zeolites by e.p.r. has been reviewed by Mikheikin[9].

SORPTION PROPERTIES :

The crystalline zeolites are widely used as selective adsorbents. They have a high sorptive capacity at low adsorbate concentration and at high temperatures. Sorption of gases on various ion exchanged forms of chabazites have been reported by Rabinowitch and Wood[10]. Barrer[11] studied sorption equilibria of ammonia on natural zeolites. The sorption kinetics revealed two types of gas uptake; rapid in chabazite and slow in platty and fibrous zeolites.

The sorption of gases like H_2, N_2 and O_2 in mordenite and chabazite have been reported in literature[12]. The pre-sorption of polar molecules such as H_2O, NH_3 in the channels of various zeolites, introduces critical changes in the subsequent sorption properties of non-polar gases[13-16]. From the sorption measurements with O_2, N_2, A and a series of n-, iso- and neo-paraffins in synthetic faujasites at different temperatures, Barrer and Sutherland[17] found that permanent gases are selectively occluded in the order of their quadrupole moment. Thus, the separation of N_2 and O_2 by molecular sieves has been

ascribed not to molecular sieve action but to the difference in sorption affinities. Barrer and co-workers[18-21] reported the influence of alkali and alkaline earth ions on the sorption phenomenon in several zeolites and concluded that zeolites in K-form behave as energetically homogenous sorbent for N_2.

Dubinin and co-workers[22] examined sorption of N_2 and H_2O on X-type zeolites. The results were found to be in agreement with the potential theory. Kiselev and associates[23-25] studied the adsorption properties of zeolites at low temperatures and low pressures.

THERMAL STABILITY OF ZEOLITES :

The modifications occurring in the zeolite framework structures on ion exchange and on thermal treatment can be evaluated from DTA, TGA, IR and electron microscopic techniques. The thermal stability of ammonium exchanged Y type zeolites have been studied extensively[26,27]. The literature[28] on DTA, TGA studies on NH_4Y indicates that the dehydroxylation temperature increases with the increase in the Si/Al ratio in the zeolite. From the thermal analysis of a series of modified chabazites, Barrer and Langley[29] found that the thermal stability increased with increase in the size of the exchanged cations.

APPLICATIONS :

The crystalline zeolites can be used for a wide variety of purposes including static and dynamic drying and selective separations of gases and liquids. The synthetic zeolites have great affinity for water and for small diameter molecules. They reject or exclude large diameter molecules. They have also a high sorptive capacity at low adsorbate concentration and at high temperatures. The zeolites generally undergo very small structural changes while they are in use. They can be regenerated and reused with relatively small loss in efficiency. Zeolites can function as carriers for a wide variety of chemical species. They are used in ion-exchange and gas chromatography.

The crystalline character and large internal surface of zeolites has been employed in the field of catalysis. The large pore zeolites of types X and Y and mordenite are mainly used as catalysts or supports. The catalytic application of zeolites have been reviewed by Venuto and Landis[30], Leach[31], Minachev[32] and others. The high activity and stability of certain large pore zeolites, after a suitable ion exchange and pre-treatment, have resulted in a wide-spread replacement of conventional catalysts. They are extensively used in petrochemical processes for cracking[33], isomerization[34], alkylation,

hydrogenation and dehydrogenation. Rareearth zeolites are used as catalysts for alkylation of aromatics with olefins[30]. Transition metal zeolites are active in polymerization of olefins[35,36], isomerization[37-39] and disproportionation of toluene[40]. CuY is used as catalyst for the oxidation of propylene[41]. Type Y zeolites are reported to be active in oxidative dehydrogenation of cyclohexane at 220°-350°K. The catalytic applications of various types of zeolites are summarized in Table-2.

As reviewed by Venuto[42] and Venuto and Landis[30], the zeolites of type X and type Y may replace the conventional catalysts for reactions such as alkylation, dealkylation, trans-alkylation, hydrogenation, dehydrogenation, isomerization cracking and various other reactions. M-Y type (M = H or cation) zeolites are used as catalysts in the alkylation of phenol[43]. Hydrogen-mordenite is used as a catalyst for trans-alkylation[44]. Alkylation of benzene[45,46] has been carried out with CaNaY and CoNaY and NdNaY at 275-325°C; it has been found that the catalytic activity depends on the amount of Na^{+} replaced and also on the Nd^{3+}, Ca^{2+} ratio. Aromatic hydrocarbons have been alkylated with different alkylating agents by using hydrogen or rare-earth forms of zeolites[47,48]. Heterocyclic compounds were alkylated with one or more

TABLE-2 : POTENTIAL MOLECULAR SIEVE CATALYST APPLICATIONS

Process	Feed/Products	Competitive features	Probable Zeolite catalyst
Catalytic reforming	Naphtha/gasoline	Activators unnecessary; gasoline with reduced sensitivity; feed pre-treatment is minimized.	Y
Alkylation	Aromatic and low olefinic streams/ valuable alkylated aromatics.	Non-corrosive; feed pre-treatment minimized.	Y
Hydro-dealkylation	Toluene/Benzene	High activity; improved selectivity.	X,Y
Hydrogenation	Benzene/ Cyclohexane	Improved resistance to S poisoning.	X,Y
Selective Hydrogenation	Straight and branched olefins/ n-alkanes and branched olefins.	Separation problems minimized.	A
Dehydrogenation	Ethylbenzene/ styrene	Improved selectivity	X,Y
Dehydration	Alcohols + Acids/ Esters	Improved rates and yields.	A
Isomerization	Light naphtha/ high-octane blending stocks	Non-corrosive; high activity and selectivity.	Mordenite Y

alkyl groups using sodium form of zeolite[49]. Low temperature alkylation of aromatic compounds was carried out in presence of rareearth zeolite 13X (0.22 wt % Na_2O, 26.5 % RE_2O_3)[50] and Rabo et al.[51] discussed the catalytic and structural properties of rare-earth exchanged Y type zeolite. Kirsch et al.[52] have studied the alkylation of iso-paraffin-olefin with REY. Zeolite Y in various cationic and decationized form is used in alkylation of toluene with methanol[53], the activity is found to be in the order, REY > HY > divalent > monovalent. The catalytic activity of the zeolite X and zeolite Y (in H or Ca form), in cumene formation[54] was found to decrease in the order CaY > HX > CaX > NaY $\simeq$ 0. Venuto et al.[55] discussed the possible relation between the unique faujasite structure and some appearant anomalies in catalysis. From the anology with the conventional alkylation catalysts together with structural features and active sites for alkylation in acidic faujasites REX, REY and HY, Venuto[56] and others visualized these zeolites as strongly acidic in nature.

From the above literature survey, it is seen that large pore zeolites (types X, Y and mordenite) may be used as catalysts in various types of organic reactions. In particular they find extensive use when sodium is replaced by alkaline-earth or other polyvalent (rareearth) ions.

In the present work a few rareearth exchanged X and Y type zeolites (further modified in some cases by ammonium exchange to convert partially into H form) are prepared. The change in their sorption properties with the sodium replacement is evaluated by measuring the rate of vapour adsorption and surface area (low temperature nitrogen adsorption). The structural changes have been studied by X-ray, infrared and thermal analyses. Catalytic activity of the zeolites prepared by ion exchange has been checked for the alkylation of benzene with ethanol.

***

CHAPTER - II : EXPERIMENTAL

EXPERIMENTAL

MATERIALS :

The binder free X type zeolite NaX, synthesized from sodium silicate, sodium aluminate and sodium hydroxide, was used in the present investigations. The Y type zeolites (SK-40) in the sodium form and SK-41 in the ammonium form were obtained from the Union Carbide Corporation (USA) and were used for the preparation of rare-earth exchanged samples. The chemical analysis showed that the SiO_2/Al_2O_3 ratio was 2.52 in X type and 4.26 in the Y type zeolite samples.

For cation exchange, a mixed rare-earth chloride (dydimium chloride) solution was used. This was prepared from AR grade dydimium oxide, supplied by M/s Indian Rare-earths Ltd. For ammonium exchange analar grade NH_4NO_3 was used. A.R. grade reagents were used for the analysis of the zeolites. The organic solvents used for sorption measurements were also of analar grade. Double distilled water (distilled over alkaline permanganate) was used for the sorption measurements.

ION-EXCHANGE :

X and Y type zeolites in the sodium form used in this investigation were found to be highly crystalline

from the X-ray diffraction patterns. The ion exchange was carried out by using 5% solution of dydimium chloride (pH = 5.8) and NH_4NO_3 solutions. The exchange was carried out at 95°C in a specially fabricated stainless steel vessel which could be closed air-tight. The hydrated zeolite powder was mixed and stirred with required quantity of the salt solution. The mixture was kept at 95°C for a period of 6-8 hours. The exchanged zeolite was then filtered, washed free of chloride or nitrate ions and dried in the air oven at 120°C for 24 hours, cooled, powdered, sieved and kept over saturated solution of ammonium chloride in a desiccator at 25°C. The zeolites of higher degree of exchanges were obtained by repeated treatments.

COMPOSITION OF THE ZEOLITE :

The zeolite powder was dissolved in 1:1 hydrochloric acid and evaporated to dryness. After dehydration at 120°C the silica was first estimated. Aluminium was then precipitated as aluminium hydroxide. For estimating aluminium in the presence of rare-earth, the latter was first precipitated as oxalate and then aluminium was estimated as usual after decomposing oxalate ions at about 500°C. Sodium was estimated by flame photometry as well as gravimetrically. The former technique was particularly employed

when the concentration of sodium in the zeolite sample was less than 2%. The ammonia content was estimated separately by Kjeldahl's method(57).

The per cent exchange of sodium and the unit cell compositions of the ion-exchanged zeolites are summarized in Table-3.

APPARATUS :

The apparatus used for nitrogen adsorption and subsequent surface area estimation is illustrated as in Fig. 2. It consists of three burettes B_1, B_2 and B_3 (B_3 is not shown in the figure), a manometer (M) and a sample bulb (S). The sample bulb S is connected next to the burette B_3. In between B_3 and S the gas reservoirs for helium and nitrogen are connected. The mercury manometer is connected in between burette B_1 and pumping system.

The burettes B_1 and B_2 consist of series of bulbs of progressively decreasing volume. The bulbs are interconnected with capillary tubings having reference marks on them. The volumes of the bulbs are determined from the weight of mercury between successive reference marks. The burette is surrounded by a water jacket. A thermo-well is provided for the measurement of the temperature of the

TABLE-3 : COMPOSITION OF ZEOLITES

Zeolite	% Exchange	% RE_2O_3	Unit cell composition
NaX	-	-	$Na_{85}(AlO_2)_{85}(SiO_2)_{107}$
RE(1)X	88.80	26.38	$Na_{9.6}RE_{21.1}(AlO_2)_{85}(SiO_2)_{107}$
RE(2)X	90.54	26.58	$Na_{8.0}RE_{21.2}(AlO_2)_{85}(SiO_2)_{107}$
RE(3)X	94.42	27.29	$Na_{4.8}RE_{21.8}(AlO_2)_{85}(SiO_2)_{107}$
RE(4)X	97.06	29.24	$Na_{2.5}RE_{23.4}(AlO_2)_{85}(SiO_2)_{107}$
$RENH_4$(1)X	97.31	28.36	$Na_{2.4}RE_{22.6}(NH_4)_{10.4}(AlO_2)_{85}(SiO_2)_{107}$
NaY	-	-	$Na_{55}(AlO_2)_{61}(SiO_2)_{131}$
REY	95.89	22.12	$Na_{2.2}RE_{17.32}(AlO_2)_{61}(SiO_2)_{131}$
$RENH_4$(1)Y	95.78	20.33	$Na_{2.25}RE_{15.93}(NH_4)_{2.71}(AlO_2)_{61.00}(SiO_2)_{131}$
$RENH_4$(2)Y	97.22	15.40	$Na_{1.55}RE_{12.08}(NH_4)_{10.34}(AlO_2)_{61}(SiO_2)_{131}$

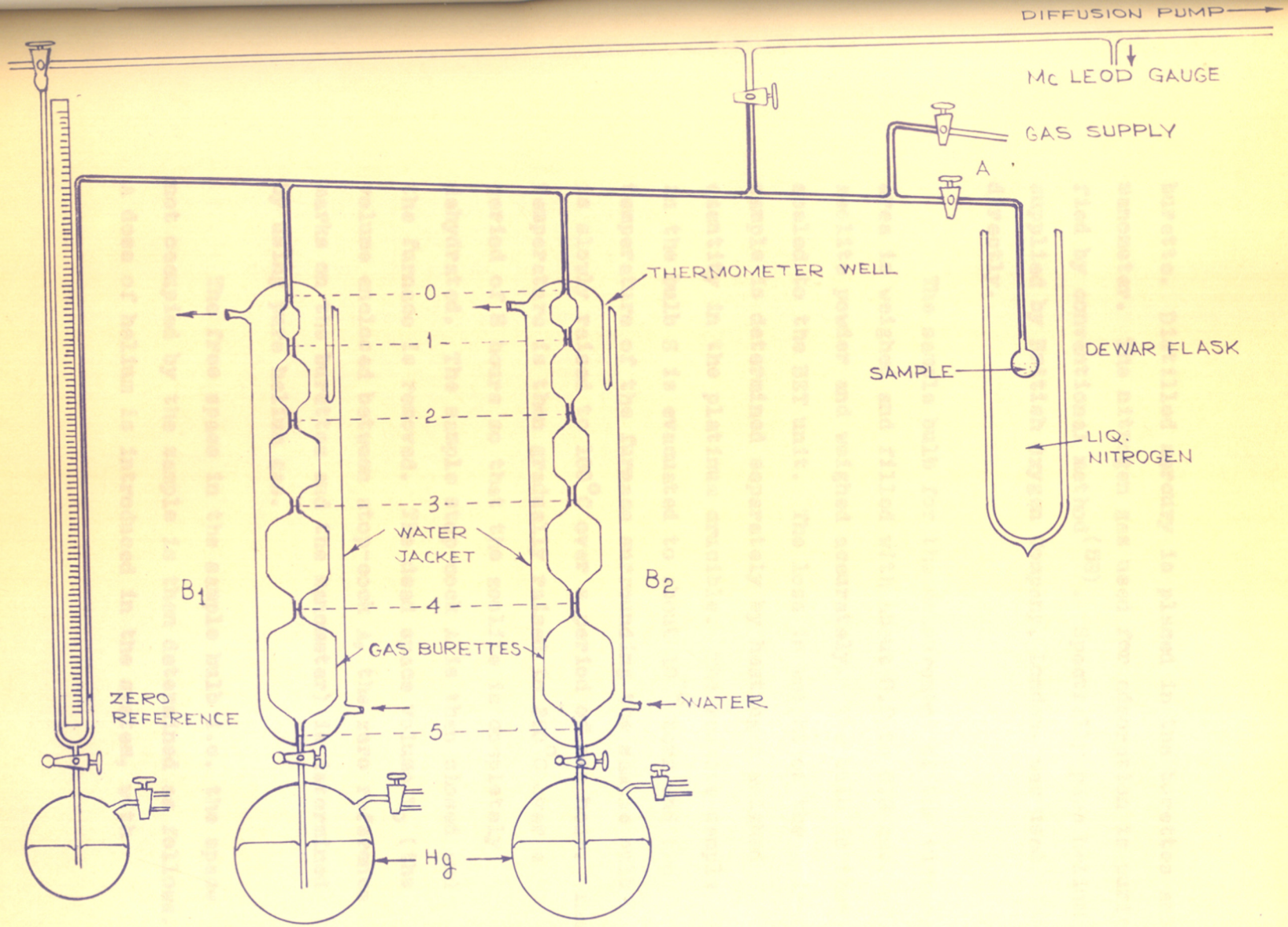

FIG.-2

GAS ADSORPTION APPARATUS FOR THE MEASUREMENTS OF BET SURFACE AREA

burette. Distilled mercury is placed in the burettes and manometer. The nitrogen gas used for adsorption is purified by conventional method[58]. Spectrally pure helium supplied by British Oxygen Company, London, was used directly.

The sample bulb for the measurement of the surface area is weighed and filled with about 0.2 to 0.3 gms. of zeolite powder and weighed accurately. The bulb is then sealed to the BET unit. The loss in weight of the hydrated sample is determined separately by heating a weighed quantity in the platinum crucible. The zeolite sample in the bulb S is evacuated to about 10^{-6} torr and the temperature of the furnace surrounding the sample bulb is slowly raised to 100°C over a period of one hour. The temperature is then gradually raised to 360°C over a period of 8 hours so that the zeolite is completely dehydrated. The sample stop-cock A is then closed and the furnace is removed. The dead space volume V_o (the volume enclosed between stop-cock A, the zero reference marks on the burettes and the manometer) is determined by using pure helium gas.

The free space in the sample bulb i.e. the space not occupied by the sample is then determined as follows. A dose of helium is introduced in the system, with

stop-cock A closed, its volume is calibrated, by compressing the gas by raising mercury to successive burette marks and noting the pressure simultaneously. The sample bulb is then immersed in liquid nitrogen bath. The stop-cock A is then opened to admit the gas in the sample bulb. Now at each reference mark, the new pressure is noted and the bulb factor (f_A) is calculated. Helium gas is then pumped off and the system is evacuated till it attains the vacuum of 10^{-6} torr. The stop-cock A is then closed. A dose of nitrogen gas is then admitted in the system and its volume is calibrated as before. Nitrogen gas is then admitted to the adsorption bulb immersed in the liquid nitrogen bath. As the gas is adsorbed by the sample the pressure in the system drops gradually. The new value of pressure is recorded when the equilibrium is established. The temperature of the burette and the position of mercury are noted. The pressure of the gas being adsorbed is increased by raising the mercury in the burettes to the successive reference marks, and the corresponding equilibrium pressures are recorded. Additional dose of nitrogen is admitted if necessary and calibrated. Adsorption measurements are carried out till requisite number of points at different pressures are obtained.

By noting the reference marks on the burettes and corresponding equilibrium pressure, the amount of gas in the adsorption bulb as well as that remaining in the system is calculated. If V_1 is the volume of nitrogen (NTP) taken in the system and V_2 is that remaining in the system upto stop-cock A and V_3 is that in the adsorption bulb, then

$$V_{adsorbed} = V_1 - V_2 - V_3 \left(1 + \frac{\alpha P}{760} \right)$$

where α is the correction for the non-ideality of nitrogen at 78°K.

The values of surface area are estimated by employing the BET and Langmuir isotherm equation respectively.

$$\frac{P}{V_{ads}(P_o - P)} = \frac{1}{V_m \cdot C} + \frac{C-1}{V_m \cdot C} \cdot \frac{P}{P_o}$$

and

$$\frac{P}{P_o \cdot V} = \frac{1}{b \cdot V_m} + \frac{P}{V_m \cdot P_o}$$

where $C = e^{(E_1 - E_2)/RT}$ = constant which depends on adsorbate-adsorbent system.

V_m = Volume of nitrogen necessary to form monolayer.

P_o = Saturated vapour pressure of nitrogen at 78°K.

If BET equation is applicable a plot of $\frac{P}{V_{ads}(P_o-P)}$ against $\frac{P}{P_o}$ should be linear with a slope $\frac{C-1}{V_m.C}$ and intercept $\frac{1}{V_m.C}$ while for Langmuir plot, $\frac{P}{P_oV}$ against $\frac{P}{P_o}$ is linear. If anhydrous weight of the sample is known the BET or Langmuir surface area can be calculated from the slope and intercept and by using the value of 16.2 $\mathring{A}^2$ for the area of nitrogen molecule.

ADSORPTION MEASUREMENTS FOR CONDENSABLE VAPOURS OF WATER AND ORGANIC SOLVENTS :

The sorption measurements for water and organic solvent vapour are conducted on a McBain-Baker type gravimetric unit (Fig. 3). A silica spring (sensitivity = 50 cms./g) is used in the gravimetric unit.

A sample bucket is suspended from a hook E on the silica spring A. The balance case is connected to the high vacuum system. The vacuum system consists of a rotary pump, mercury diffusion pump, cold traps and McLeod gauge for measuring the pressure. The burette (F) containing the adsorbate liquid is connected between balance case and the manometer (H) which is used for measuring the equilibrium pressure of the adsorbate. The adsorbate liquid is made free from air by freeze-thaw technique. Two separate thermostats G and C are used for maintaining constant temperatures for the sorbate liquid and the balance case respectively. All the stop-cocks

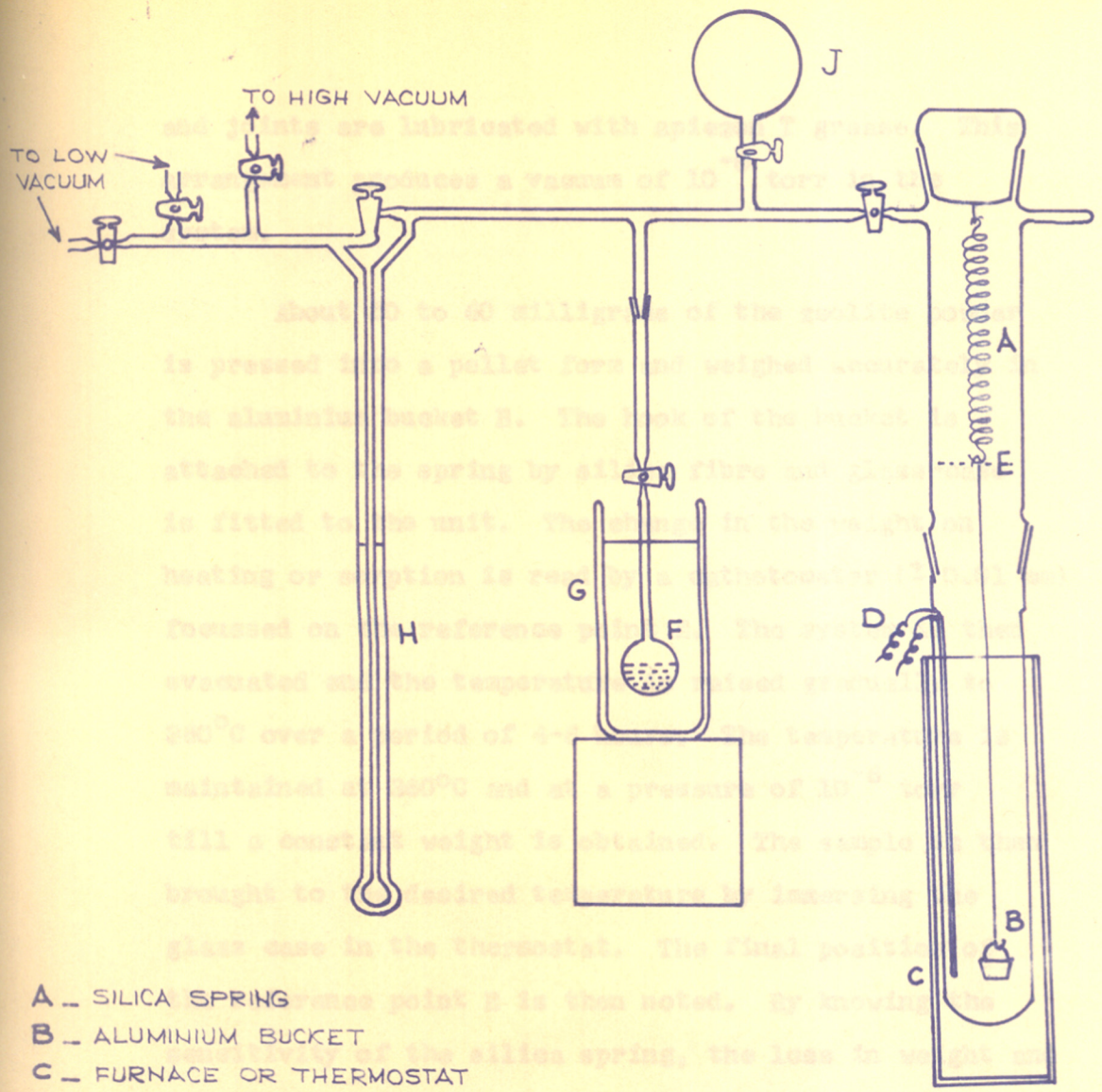

A _ SILICA SPRING
B _ ALUMINIUM BUCKET
C _ FURNACE OR THERMOSTAT
D _ THERMOCOUPLE
E _ REFERENCE POINT
F _ LIQUID BULB
G _ THERMOSTAT
H _ MANOMETER
J – GAS RESERVIOR

FIG - 3

GRAVIMETRIC ADSORPTION UNIT

and joints are lubricated with apiezon T grease. This arrangement produces a vacuum of 10^{-6} torr in the system.

About 50 to 60 milligrams of the zeolite powder is pressed into a pellet form and weighed accurately in the aluminium bucket B. The hook of the bucket is attached to the spring by silica fibre and glass-case is fitted to the unit. The change in the weight on heating or sorption is read by a cathetometer ($\pm$ 0.01 mm) focussed on the reference point E. The system is then evacuated and the temperature is raised gradually to 360°C over a period of 4-6 hours. The temperature is maintained at 360°C and at a pressure of 10^{-6} torr till a constant weight is obtained. The sample is then brought to the desired temperature by immersing the glass case in the thermostat. The final position of the reference point E is then noted. By knowing the sensitivity of the silica spring, the loss in weight and the anhydrous weight are estimated. The sample is then exposed to the adsorbate vapour from the bulb (F), at constant temperature. The sorption rate is obtained by noting change in weight with time till a constant weight or equilibrium is attained. The sample is again reactivated as described above and the sorption measurements are carried out with other sorbates in a similar manner.

X-RAY :

X-ray powder diffraction patterns of hydrated zeolite powder (300 mesh) were obtained on a Phillips X-ray unit using a 14.32 cm. diameter Debye-Scherrer camera at room temperature using CuK_{α} radiation (λ = 1.54 Å). All the zeolites were found to be highly crystalline even after exchange.

TGA AND DTA :

The thermal stability of exchanged zeolites is studied by recording the thermograms on an automatic unit MOM-Budapest Derivatograph (Type OO-102) B described by Paulick et al.[59] About 200 milligrams of powdered zeolite was used for the thermal analysis, Al_2O_3 was used as an inert material. The heating rate was 10°C per minute.

INFRARED SPECTRA :

The IR spectra were recorded in the frequency range of 320 to 714 cm^{-1} using Perkin-Elmer 221 spectrometer. The nujol-mull of hydrated samples were used for recording the spectra.

CATALYTIC STUDIES - ALKYLATION - REACTOR ASSEMBLY :

The catalytic activity and the active life of the exchanged zeolites for the alkylation of benzene with

ethanol is studied using a reactor assembly shown in the Figure 4.

The preheater (P) is made of pyrex glass of about 1.5 cm. wide and 30-40 cm. long and is filled with inert porcelain beads. The reactor (R) is also made of pyrex and has the same dimension as that of the preheater. The reactor is first filled (1/4) with porcelain beads and then (upto 3/4) with the catalyst and again with the porcelain beads. The receiver is connected to the reactor through a double walled condenser for condensing the vapours of reaction products. Gasous bye-products are allowed to escape through a bubbler. The thermocouples in the thermo-wells are connected to calibrated temperature indicators for recording the temperatures of the preheater and the reactor. Electrical heaters are wound around both preheater and reactor and are connected to the mains through the variac. Two thermo-wells are provided along the centre of the preheater and the reactor.

CATALYST :

The powdered catalyst zeolite is mixed with suitable binder in the required proposition and extruded to (3/16") size pellets. The pellets are dried at 120°C for 24 hours and are activated in the furnace at 500°C for 4 hours, cooled and equilibrated in the air and are cut into 4-5 mm in length. 10 grams of pellets are charged in the reactor.

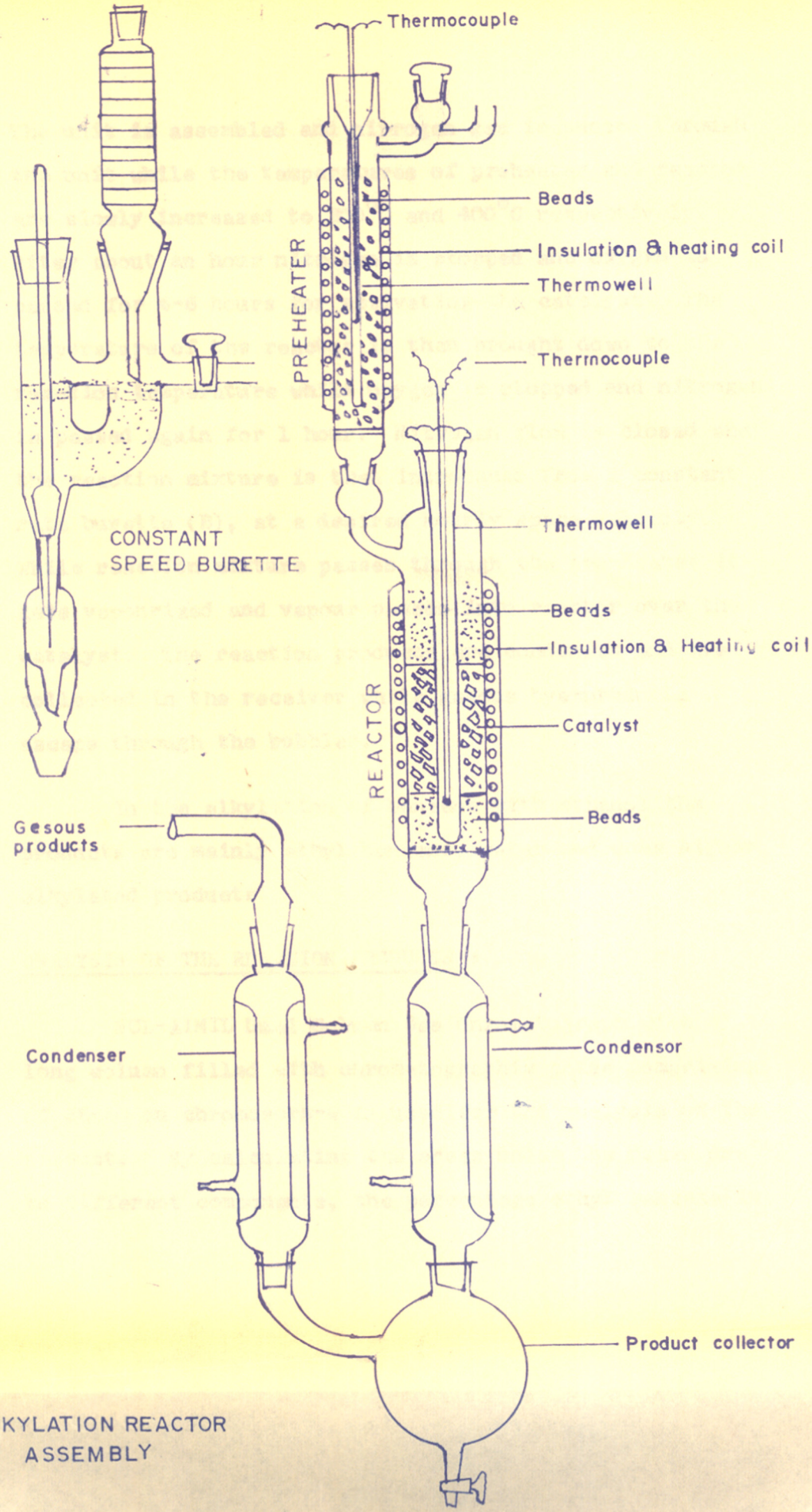

FIG. 4. ALKYLATION REACTOR ASSEMBLY

The unit is assembled and nitrogen gas is passed through the unit while the temperatures of preheater and reactor are slowly increased to 200°C and 400°C respectively. After about an hour nitrogen is stopped and oxygen is passed for 4-6 hours for activating the catalyst. The temperature of the reactor is then brought down to the reaction temperature while oxygen is stopped and nitrogen is passed again for 1 hour. Nitrogen flow is closed and the reaction mixture is then introduced from a constant rate burette (B), at a desired hourly space velocity. While reaction mixture passes through the pre-heater it gets vapourized and vapour passes into reactor over the catalyst. The reaction products are condensed and are collected in the receiver while gasous bye-products escape through the bubbler.

In the alkylation of benzene with ethanol the products are mainly ethyl benzene, water and some higher alkylated products.

ANALYSIS OF THE REACTION PRODUCTS :

NCL-AIMIL Dual Column Gas Chromatograph with 8' long column filled with chromatographic phase comprising of SE-30 on chromosorb-W is used for the analysis of the products. By calculating the areas under the peaks due to different components, the percentage ethyl benzene in

the product and the percentage conversion is calculated. For the accurate calculations of areas under the curves, the GLC of mixtures of benzene, alcohol and ethyl benzene of known composition are determined and the corresponding factors are calculated.

***

CHAPTER - III : RESULTS AND DISCUSSION

RESULTS AND DISCUSSION

The catalytic sorption and other physicochemical properties of zeolites depend on the chemical composition of their skeleton and the geometry of the openings of the chennels in the porous crystals[60-62]. Cations play an important role in the sorption properties. Within one type of zeolite the adsorption and other properties are determined to a certain extent by the nature of the cation, their number per unit cell and by the degree of population of single centre in the crystal framework. The results obtained on such studies are discussed in the following.

ADSORPTION OF NITROGEN :

The sorption of nitrogen has been studied at 78°K./90°K The results are summarized in Table-4 and are represented in Figures 5 and 6. It is seen that the sorption capacity of both zeolites type X and Y decreases with the progressive substitution of RE^{3+} ions for Na^{+} ion and follows the order NaX > RE(1)X > RE(2)X > RE(3)X > $RENH_4X$ > RE(4)X ; while NaX sorbs 222.8 ml (NTP) per gram anhydrous zeolite, RE(4)X sorbs only 178.0 ml nitrogen at pressure of 500 torr.

A similar trend is also observed in case of Y type zeolites. NaY sorbs about 235.0 mls. of nitrogen at

TABLE-4 : NITROGEN ADSORBED (mls/g) AT 78°K

Pressure in mm.	N_2-Adsorption									
	NaX	RE(1)X	RE(2)X	RE(3)X	RE(4)X	$RENH_4X$	NaY	REY	$RENH_4(2)Y$	$RENH_4(1)Y$
20	210.0	180.5	177.5	175.0	167.0	170.0	221.0	181.50	204.5	181.5
40	216.0	184.0	182.0	179.5	169.7	173.2	225.0	185.5	208.0	185.5
60	219.5	186.5	184.2	182.2	171.2	175.0	227.2	188.0	209.5	188.0
100	221.0	188.0	186.5	184.5	173.5	176.7	229.0	192.0	211.0	192.0
150	221.0	189.0	187.0	185.5	175.0	178.0	229.7	194.5	212.0	194.0
200	221.2	190.0	188.0	185.7	175.7	179.0	230.7	195.2	212.5	194.5
250	221.5	190.7	188.2	186.0	176.0	179.5	231.5	196.0	213.0	195.2
300	221.7	191.2	188.5	186.2	176.5	179.7	232.0	196.5	213.5	195.7
350	222.0	191.7	188.7	186.5	176.7	180.0	232.5	197.2	213.7	196.2
400	222.2	192.2	189.0	186.7	177.2	180.2	233.0	198.0	214.0	197.0
450	222.5	193.0	189.5	187.0	177.5	180.3	234.0	198.7	214.5	197.5
500	222.7	193.5	190.0	187.5	178.0	180.5	234.5	199.5	215.0	198.0

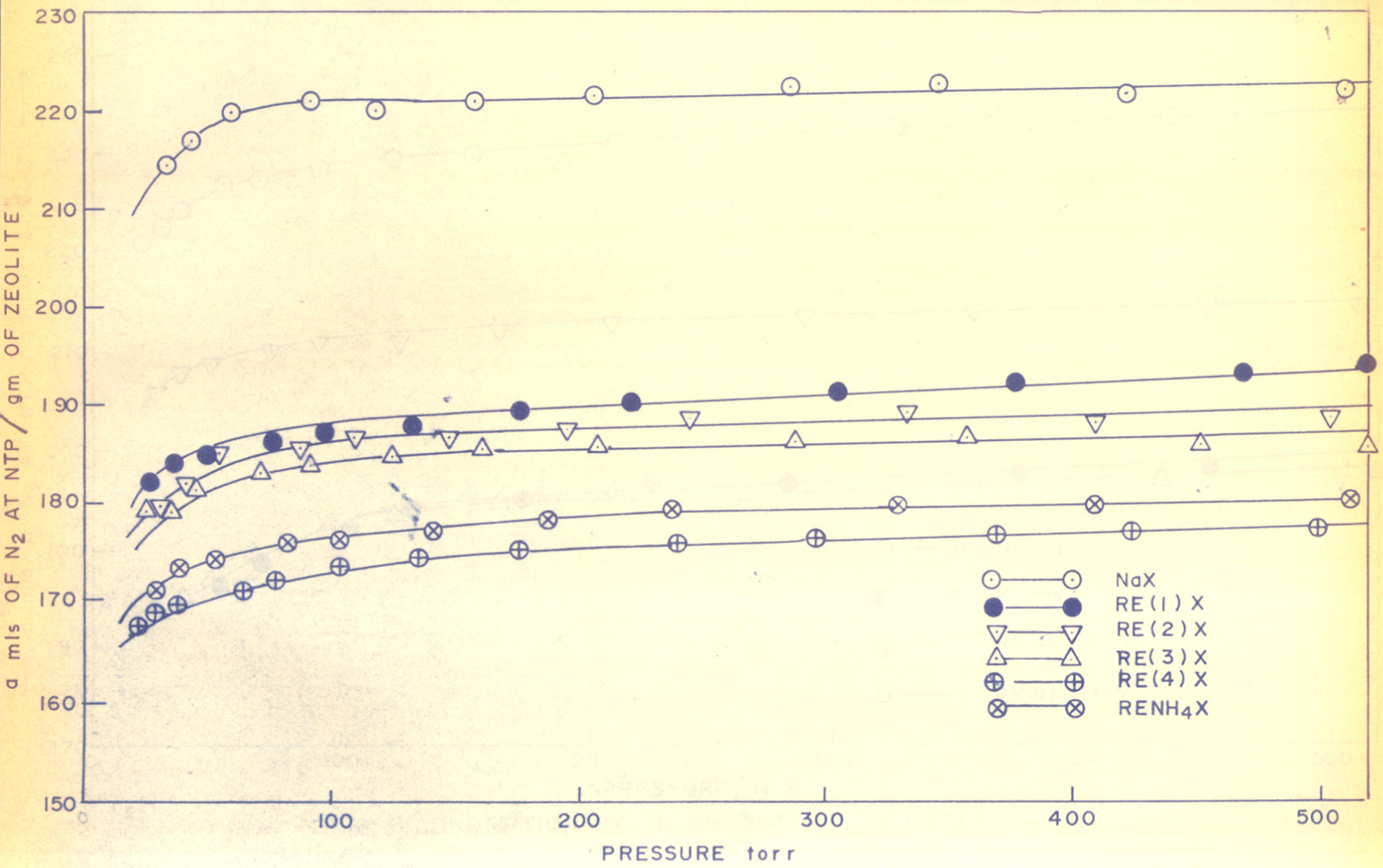

FIG. 5. ADSORPTION OF N_2 ON X TYPE ZEOLITES

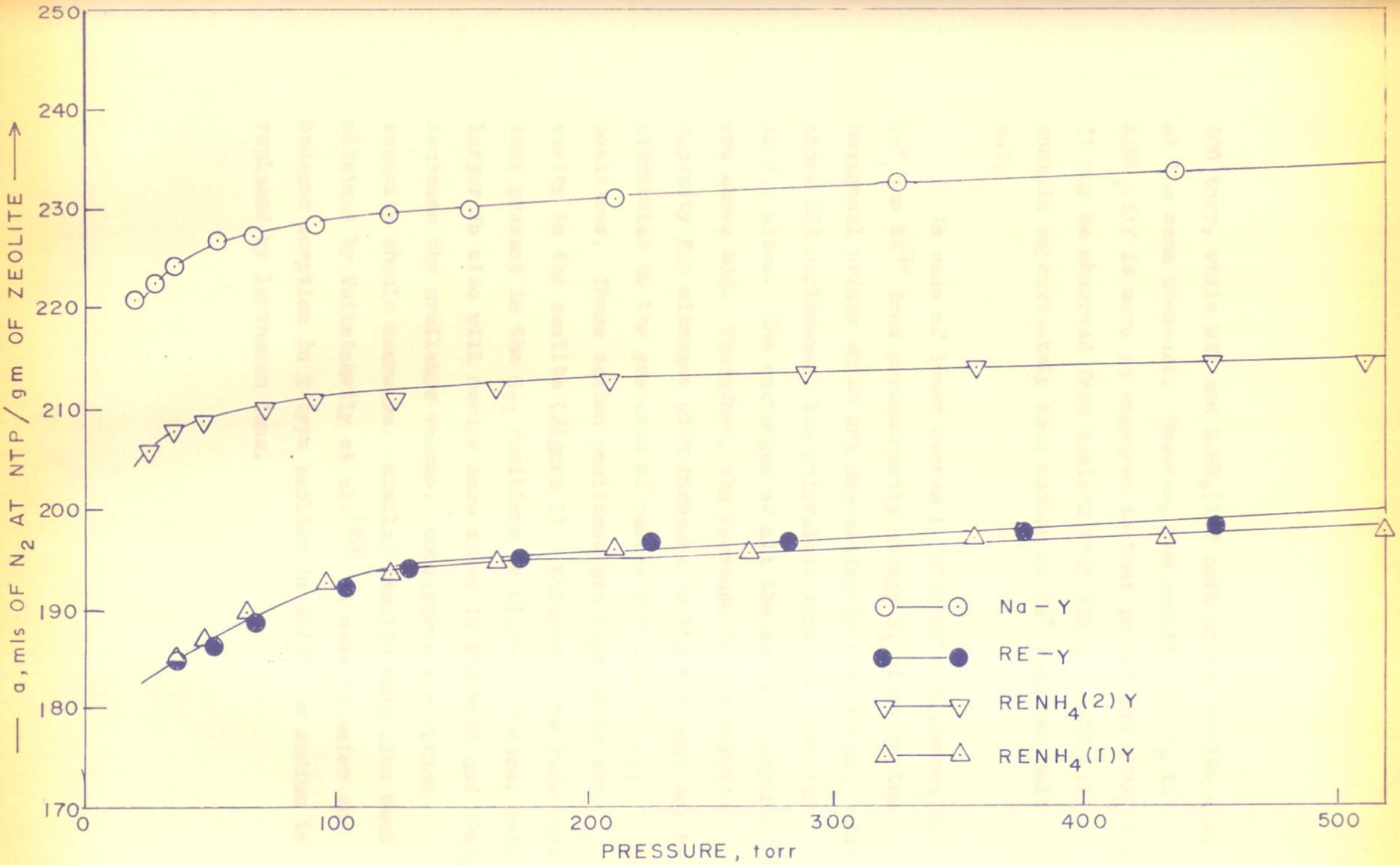

FIG. 6. ADSORPTION OF N_2 ON Y TYPE ZEOLITES

500 torr, while REY and $RENH_4(1)Y$ sorb about 198-199 mls. at the same pressure. However, the sorption of N_2 in $RENH_4(2)Y$ is more as compared to that in REY and $RENH_4(1)Y$. It may be observed from Table-3 that REY and $RENH_4(1)Y$ contain approximately same number of Na^+ ions per unit cell.

In case of lower degree ($<60\%$) of replacement of Na^+, the RE^{3+} ions predominantly occupy S_I sites in the hexagonal prisms which are energetically favourable. While above 60% replacement the polyvalent ions are situated in S_{II} sites. The exchanges of all the samples prepared are above 80%. Therefore, the decrease in the sorption capacity for nitrogen with increase in the exchange may be attributed to the presence of rare-earth ions in S_{II} positions. These cation positions are exposed to the cavity in the zeolite (Figure 1). Moreover, the rare-earth ions present in the S_{II} positions in place of sodium, being larger in size will occupy more space in the void and thus, decrease the available volume. Consequently sorption capacity should decrease. Similar results have also been obtained by Tsitsishvily et al.[63] in case of water and benzene sorption in X type zeolite in which the sodium is replaced by lanthanum ions.

The sorption capacity of $RENH_4X$ is slightly more than for RE(4)X although the number of Na^+ ions per unit cell in both the samples is nearly the same. The sorption capacity of $RENH_4$(2)Y having relatively smaller number of sodium ions per unit cell as compared to $RENH_4$(1)Y is higher. This could be attributed to the presence of larger number of NH_4^+ (H^+) ions in the zeolite. The replacement of Na^+ in type Y zeolite by smaller NH_4^+ ions which are subsequently reduced to hydrogen ions by calcination increases sorptive capacity of the zeolite[64].

From the above results it may be concluded that high degree of sodium replacement by rare-earth ions is operative in decreasing sorption capacity, while replacement of sodium by hydrogen might be operative in increasing the sorption capacity of the zeolites provided the crystalline nature of the zeolite lattice is retained. Therefore, there seems to be a compromise in both the tendencies in the samples containing both rare-earth ions and hydrogen ions. This may explain the higher sorptive capacity of $RENH_4X$ as compared to RE(4)X with the same percentage exchange. Similarly the sorption capacity of $RENH_4$(2)Y is more than that of $RENH_4$(1)Y as the latter contains more hydrogen ions. Finally, it may be noted that even with 97.6% exchange of Na^+ with RE^{3+} and NH_4^+ ions, the crystal structure remains intact (Figures 21 and 22).

LANGMUIR, BET AND H.-J. ADSORPTION ISOTHERMS :

An adsorption isotherm shows how the amount of the adsorbed gas depends upon the equilibrium pressure of the gas at constant temperature. Several isotherm equations have been derived to represent the experimental data. The Langmuir equation is based on the concept of a monomolecular adsorption while Brunauer-Emmett-Teller (BET) approach is based on multilayer adsorption. The Harkins-Jura equation is based on the assumption that the adsorbed gas forms a condensed two-dimensional film on the solid surface. The Langmuir, BET and Harkins-Jura isotherm equations may be expressed by equations 1, 2 and 3 respectively.

$$\frac{P}{V.P_o} = \frac{1}{b.V_m} + \frac{P}{V_m.P_o} \qquad \ldots\ldots (1)$$

$$\frac{P}{V(P_o-P)} = \frac{1}{V_m.C} + \frac{C-1}{V_m.C}\frac{P}{P_o} \qquad \ldots\ldots (2)$$

$$\ln \frac{P}{P_o} = D - \frac{C}{V^2} \qquad \ldots\ldots (3)$$

where P = Equilibrium pressure,

P_o = Saturated vapour pressure of nitrogen at 78°K, 198K

V_m = Volume of the sorbate gas necessary to form monolayer on the sorbent,

b, C and D are constants. If the Langmuir equation is applicable, a plot of $\frac{P}{P_oV}$ against $\frac{P}{P_o}$ should give a

straight line, while for BET approach the plot of $\frac{P}{V(P_o-P)}$ against $\frac{P}{P_o}$ is linear. According to H.-J. equation a linear relation between ln $\frac{P}{P_o}$ against $\frac{1}{V^2}$ confirms its applicability to the adsorption process.

SURFACE AREA ESTIMATION :

The estimation of the number of molecules of the adsorbate to form a monomolecular layer on the surface (external as well as internal) per gram of the sample gives the measure of the surface area of the adsorbent provided the area occupied by a single adsorbate molecule is known. Typical Langmuir and BET plots made according to equations (1) and (2) are shown in Figures 7 and 8 for NaX (at 90°K) and NaY at 78°K respectively. Each of these plots show linear relation for the Langmuir isotherm upto pressure range of 400-500 torr while in the same pressure range the BET plots are non-linear. Similar plots are reported by Hopper[65] in case of surface area determination with nitrogen at 78°K in Pd-mordenite ($SiO_2/Al_2O_3 = 9$). The nitrogen sorption in other rare-earth exchanged zeolites also exhibit similar behaviour. These results indicate that the nitrogen adsorption in zeolites takes place in accordance with the Langmuir approach. The Table-5 lists the values of amount of nitrogen necessary to form monolayer according to BET and Langmuir

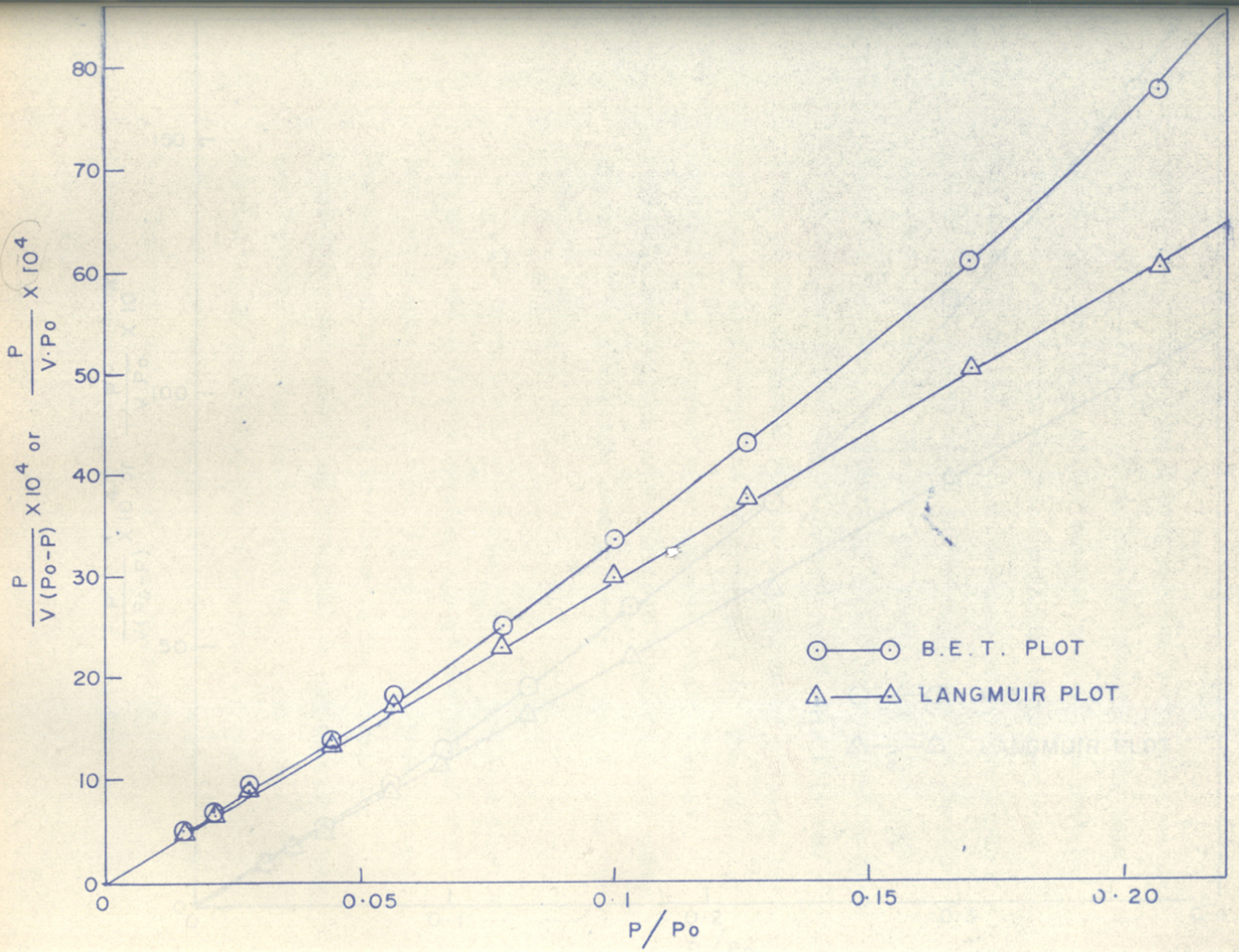

FIG. 7. B.E.T. AND LANGMUIR PLOTS FOR NaX ZEOLITE
(NITROGEN ABSORPTION AT -183 °C)

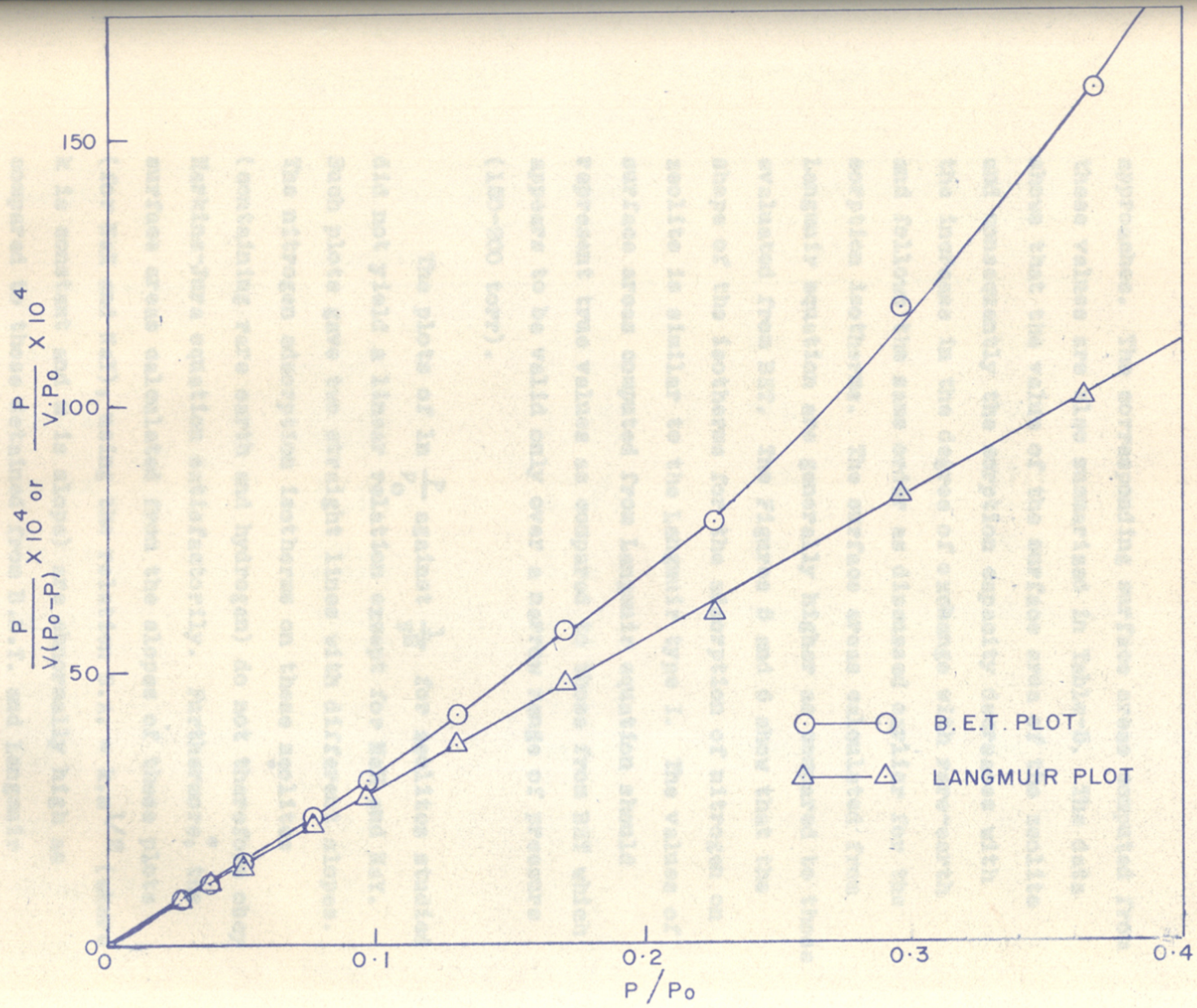

FIG. 8. B.E.T. AND LANGMUIR PLOTS FOR Na-Y ZEOLITE
(NITROGEN ABSORPTION AT −195°C)

approaches. The corresponding surface areas computed from these values are also summarized in Table-5. The data shows that the value of the surface area of the zeolite and consequently the sorption capacity decreases with the increase in the degree of exchange with rare-earth and follows the same order as discussed earlier for the sorption isotherms. The surface areas calculated from Langmuir equation are generally higher as compared to those evaluated from BET. The Figures 5 and 6 show that the shape of the isotherms for the adsorption of nitrogen on zeolite is similar to the Langmuir type I. The values of surface areas computed from Langmuir equation should represent true values as compared to those from BET which appears to be valid only over a narrow range of pressure (150-200 torr).

The plots of $\ln \frac{P}{P_o}$ against $\frac{1}{V^2}$ for zeolites studied did not yield a linear relation except for NaX and NaY. Such plots gave two straight lines with different slopes. The nitrogen adsorption isotherms on these zeolites (containing rare earth and hydrogen) do not therefore obey Harkins-Jura equation satisfactorily. Furthermore, the surface areas calculated from the slopes of these plots (for NaX and NaY), using the relation $S.A. = k.m^{1/2}$ (where k is constant and m is slope) are abnormally high as compared to those detained from B.E.T. and Langmuir approaches (Table-5).

TABLE-5 : SATURATION CAPACITY AND THE SURFACE AREAS OF DIFFERENT ZEOLITES

Zeolite	V_m in mls/g (m Moles/g)*		Surface area (m^2/g)	
	Langmuir	BET	Langmuir	BET
NaX	221.6 (9.89)	204.7 (9.14)	970.6	896.6
RE(1)X	192.9 (8.61)	178.8 (7.98)	844.7	783.2
RE(2)X	187.9 (8.39)	186.6 (8.33)	823.1	817.4
RE(3)X	187.2 (8.36)	178.2 (7.96)	820.0	780.6
RE(4)X	176.0 (7.86)	173.0 (7.72)	769.5	758.0
$RENH_4X$	180.7 (8.07)	175.6 (7.84)	791.3	769.0
NaY	234.0 (10.45)	213.6 (9.54)	1024.7	936.7
REY	200.0 (8.93)	170.6 (7.62)	876.0	747.3
$RENH_4(2)Y$	215.2 (9.61)	189.1 (8.44)	942.5	828.3
$RENH_4(1)Y$	194.0 (8.66)	166.7 (7.44)	849.7	730.0

* Bracketed figures denote saturation capacities in m Moles/g.

LANGMUIR COEFFICIENT :

The simplest isotherm equation describing localized sorption of molecules on sites which are independent of each other and are energetically equivalent, is that of Langmuir. At an equilibrium pressure P,

$$P = K_1 \left(\frac{\theta}{1-\theta} \right) \qquad \ldots\ldots (4)$$

where θ is the fraction of the surface covered and is estimated as the ratio of V/V_s where V is the amount adsorbed and V_s is the saturation capacity. The original Langmuir equation has been modified[17] to explain various physical properties of the sorbed phase. Tables 6 and 7 give the values of K_1 at different values of θ for various zeolites. From the Tables 6 and 7 it is seen that K_1 increases with θ in the range 0.95-0.97 and then it decreases. Similar results were obtained by Barrer and Sutherland[17] in case of butane adsorption by different faujasites. The plot of log K_1 against θ is linear over a range of θ = 0.9 - 0.95. The Langmuir equation has been applied[66] to the sorption of nitrogen/methane mixtures in 4A and that of benzene at 150-200°C in decationized type Y zeolite[67].

FREE ENERGY OF SORPTION :

Adsorption is an exothermic process and it takes place with a decrease in the surface free energy ΔG°. The

TABLE-6 : LANGMUIR COEFFICIENT FOR X TYPE ZEOLITES

Pressure mms	Zeolites											
	NaX		RE(1)X		RE(2)X		RE(3)X		RE(4)X		$RENH_4X$	
	θ	K_1	θ	K_1	θ	K_1	θ	K_1	θ	K_1	θ	K_1
20	0.948	1.10	0.936	1.37	0.944	1.18	0.935	1.40	0.949	1.07	0.941	1.25
40	0.975	1.03	0.954	1.92	0.968	1.31	0.959	1.72	0.965	1.47	0.952	2.02
60	0.991	0.57	0.967	2.05	0.980	1.20	0.973	1.64	0.973	1.65	0.969	1.94
100	0.997	0.27	0.975	2.59	0.992	0.77	0.985	1.48	0.986	1.43	0.978	2.21
150	0.997	0.41	0.980	3.06	0.995	0.75	0.991	1.39	-	-	0.985	2.24
200	0.998	0.32	0.985	3.26	-	-	0.992	1.59	-	-	0.991	1.86
250	-	-	0.989	2.76	-	-	0.993	1.66	-	-	0.994	1.61
300	-	-	0.992	2.54	-	-	0.995	1.60	-	-	0.995	1.51

TABLE-7 : LANGMUIR COEFFICIENT FOR Y TYPE ZEOLITES

Zeolites							
NaY		REY		$RENH_4(2)Y$		$RENH_4(1)Y$	
θ	K_1	θ	K_1	θ	K_1	θ	K_1
0.9446	1.17	0.9075	2.02	0.9503	1.04	0.9356	1.38
0.9617	1.59	0.9275	3.13	0.9666	1.38	0.9562	1.83
0.9713	1.77	0.9400	3.83	0.9735	1.63	0.9691	1.91
0.9788	2.17	0.9600	4.17	0.9805	1.99	0.9897	1.04
0.9820	2.75	0.9725	4.24	0.9852	2.25	-	-
0.9863	2.77	0.9763	4.85	0.9875	2.53	-	-
0.9895	2.65	0.9800	5.10	0.9898	2.58	-	-
0.9916	2.54	0.9825	5.34	0.9921	2.39	-	-
0.9938	2.18	0.9863	4.86	0.9933	2.39	-	-
0.9959	1.65	0.9900	4.04	0.9944	2.25	-	-

differential free energy of adsorption is given by

$$+\Delta G^{\circ} = -RT \ln P/P_{o} = RT \ln P_{o}/P \quad \ldots\ldots (5)$$

where P_{o} is the saturated vapour pressure and P is the equilibrium pressure.

The free energy of sorption for varying amounts of nitrogen adsorbed (the surface coverage), at different relative pressures, are summarized in Tables 8 and 9. It is observed that the values of ΔG° decrease with increased surface coverages and at a given value of ΔG°, the sorption decreases with the exchange of sodium with RE^{3+} and RE^{3+} & H^{+} ions. From the Tables 8 and 9 it is seen that the system attains a more stable state as the θ approaches to unity. The i.r. spectra of the framework structure and the DTA studies discussed later also indicate increased stability of the zeolite lattice with progressive exchange of Na^{+} for RE^{3+} and H^{+} ions.

VOID VOLUME CALCULATIONS - DUBININ EQUATION :

The empirical relation between the free energy of adsorption RT ln (P_{o}/ P) and the volume of adsorption space W is based on Polanyi potential theory. The Polanyi adsorption equation has been modified by Dubinin and Randushkevich[68] and may be expressed as

$$W = W_{o}\ e^{-kA^{2}/\beta^{2}} \quad \ldots\ldots (6)$$

TABLE-8 : ΔG° VALUES FOR ZEOLITE-N_2 SYSTEM AT 78°K 90°K

P/P_o	ΔG° Cals./mole	Amount adsorbed (mls./g.)					
		NaX	RE(1)X	RE(2)X	RE(3)X	RE(4)X	$RENH_4X$
0.00982	825.0	210.0	180.50	177.50	175.00	167.00	170.00
0.01964	700.4	216.0	184.00	182.00	179.50	169.25	173.25
0.02947	628.2	219.5	186.50	184.25	182.25	171.25	175.00
0.04911	537.1	221.0	188.00	186.50	184.50	173.50	176.25
0.07367	464.9	221.0	189.00	187.00	185.50	175.00	178.00
0.09822	413.6	221.25	190.00	188.00	185.75	175.75	179.00
0.12278	373.8	221.50	190.75	188.25	186.00	176.00	179.50
0.14734	341.2	221.75	191.25	188.50	186.25	176.50	179.75
0.17190	313.8	222.00	191.75	188.75	186.50	176.75	180.00
0.19645	287.5	222.25	192.25	189.00	186.75	177.25	180.20
0.22100	269.1	222.50	193.00	189.50	187.00	177.50	180.30
0.24556	250.2	222.75	193.50	190.00	187.50	178.00	180.50

TABLE-9 : ΔG° VALUES FOR ZEOLITES-N_2 SYSTEM AT 78°K

P/P_o	ΔG° Cals./mole	Amount adsorbed (mls./g.)			
		NaY	REY	$RENH_4(2)Y$	$RENH_4(1)Y$
0.02805	513.9	221.00	181.50	208.00	181.50
0.05610	414.2	225.00	185.50	208.00	185.50
0.08415	355.9	227.25	188.00	209.50	188.00
0.14025	282.4	229.00	192.00	211.00	192.00
0.21038	224.4	229.75	194.50	212.00	194.00
0.28050	182.8	230.75	195.25	212.50	194.50
0.35063	150.7	231.50	196.00	213.00	195.25
0.42075	124.5	232.00	196.50	213.50	195.75
0.49088	102.3	232.50	197.25	213.75	196.25
0.56100	83.1	233.00	198.00	214.00	197.00
0.63113	66.2	234.00	198.75	214.50	197.50
0.70125	51.0	234.50	199.50	215.00	198.00

where W is the volume occupied by the sorbed phase at a given temperature T and pressure P. The equation (6) may be written as

$$W = W_o \exp\left[-\frac{B}{\beta^2}\left(T \log_o \frac{P_s}{P}\right)^2\right] = a\,V^* \qquad \ldots\ldots (7)$$

where W_o is the constant and represents the volume of the adsorption space or pore volume and B is a constant which is independent of temperature and is characteristic of pore structure. β is called the "affinity coefficient". Below the boiling point of the liquid, V^* is taken as the molar volume of the liquid. The above equation may be put into the form

$$\log W = \log W_o - \frac{B}{2.303\,\beta^2}\left(T \log \frac{P_s}{P}\right)^2 \qquad \ldots\ldots (8)$$

$$\log (a) = C - D\left(\log \frac{P_s}{P}\right)^2 \qquad \ldots\ldots (9)$$

where C and D are constants given by equations (10) and (11). The plot of log (a) against $\left(\log \frac{P_s}{P}\right)^2$ should give a straight line with intercept

$$C = \log \frac{W_o}{V^*} \qquad \ldots\ldots (10)$$

and a slope

$$D = \frac{0.434\ BT^2}{\beta^2} \qquad \ldots\ldots (11)$$

The typical plots of log (a_s) against (log $\frac{P_s}{P}$)^2 for the sorption of nitrogen in X and Y type zeolites are shown in the Figures 9 and 10. The data indicates that the Dubinin equation is applicable over a wide range of pressures in both X and Y type zeolites in rare-earth and hydrogen forms. The saturation values (a_s) obtained from the intercepts of these straight lines are summarized in Table-10.

There are two types of voids in X and Y type zeolites, large voids which accommodate large molecules in addition to small molecules and small voids which accommodate only small polar molecules, such as water, ammonia etc. If (a_s) is the saturation capacity and d_t is the density of the adsorbate at temperature t°C, then the total void volume V_p is expressed as

$$V_p = \frac{a_s}{d_t} \qquad \ldots\ldots (12)$$

The total void volumes V_p calculated for both X and Y type zeolites are given in Table-10. The void volume of NaX as determined from nitrogen adsorption is 0.36 cm^3/g.

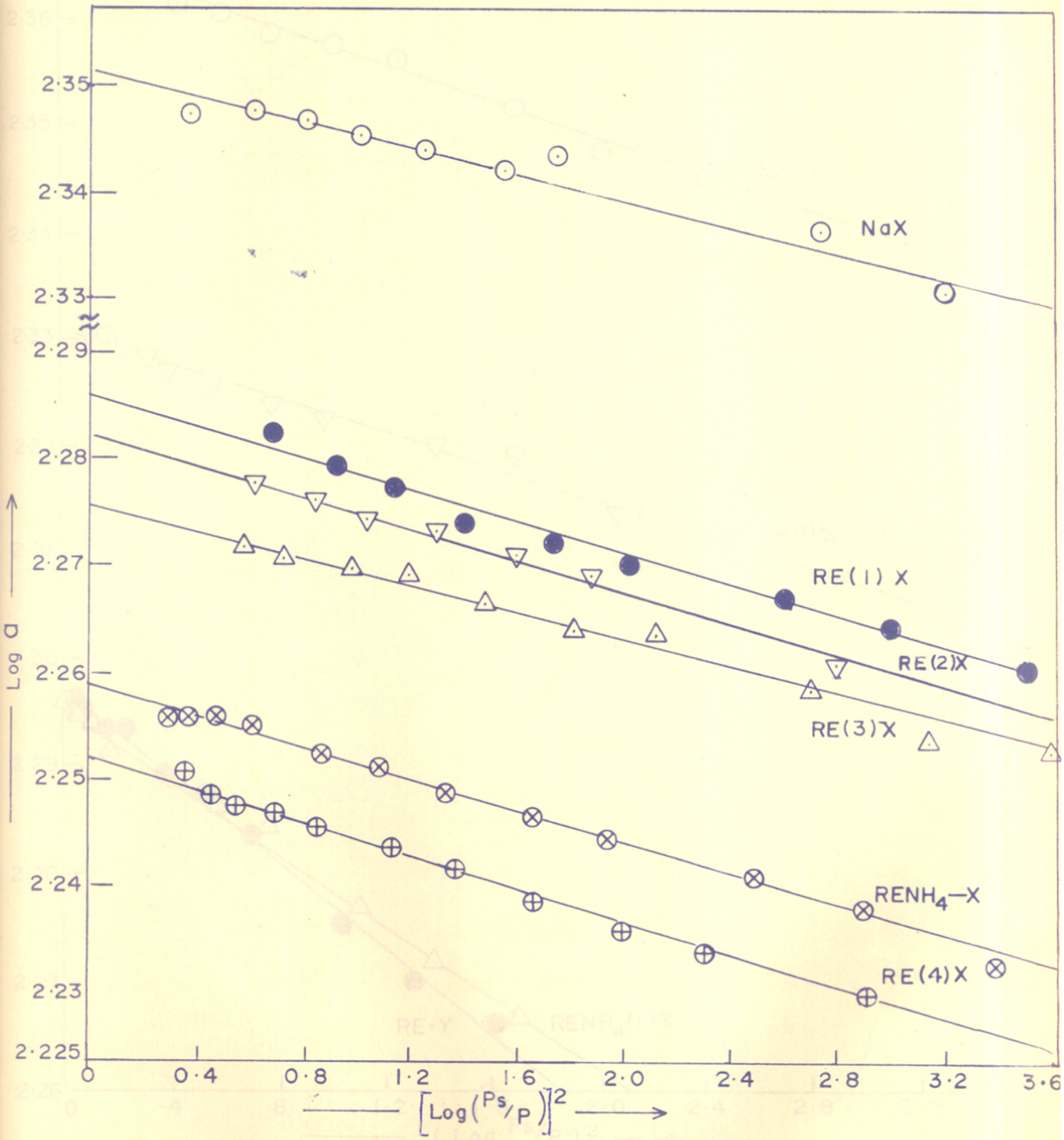

FIG. 9 . DUBININ PLOTS FOR THE ADSORPTION OF NITROGEN ON X TYPE ZEOLITES

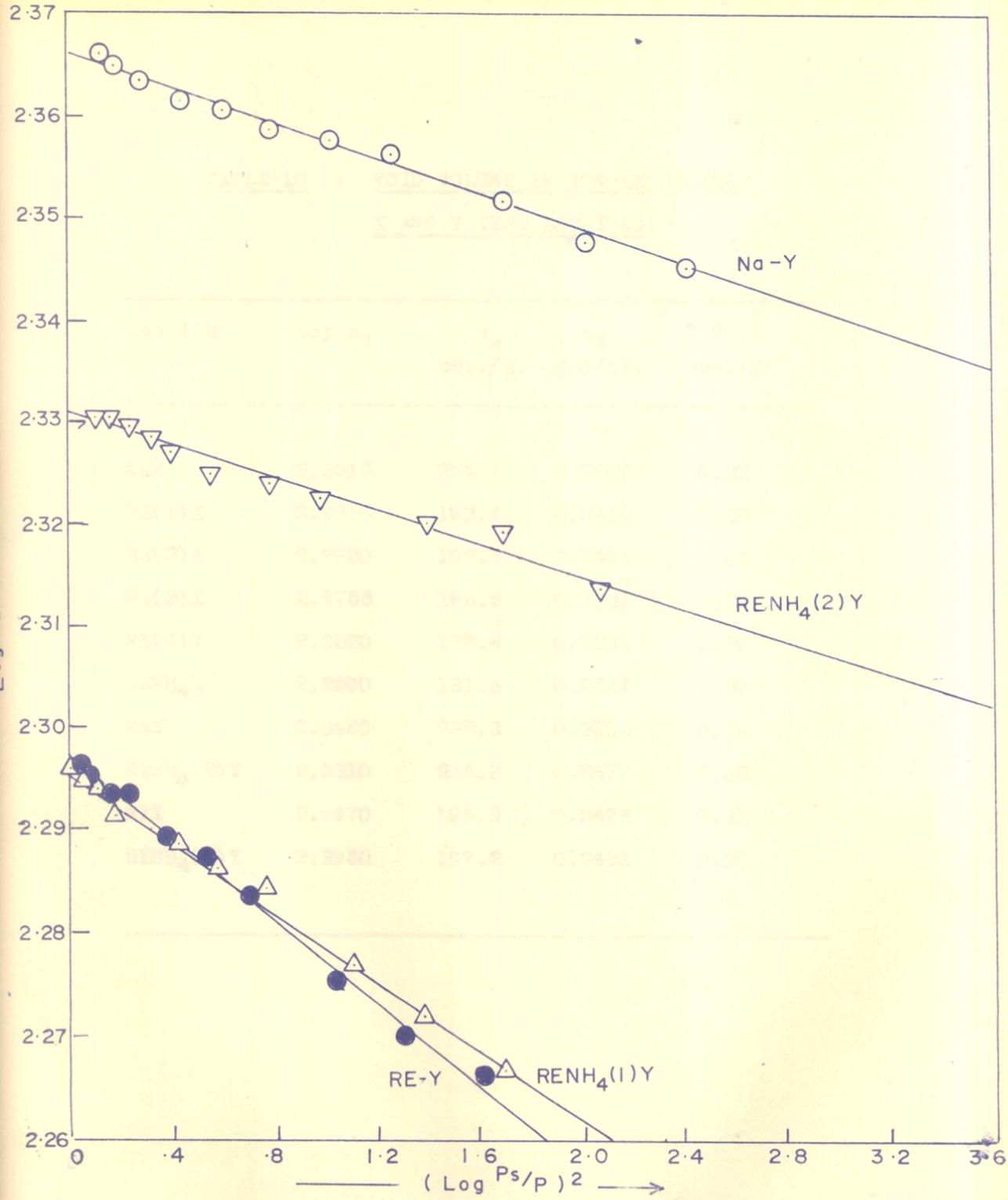

FIG.10. DUBININ PLOTS FOR THE ADSORPTION OF NITROGEN ON Y TYPE ZEOLITES

TABLE-10 : VOID VOLUME IN ION-EXCHANGED X AND Y TYPE ZEOLITES

Zeolite	Log a_s	a_s ccs./g.	a_s gms/gm.	V_p ccs./g.
NaX	2.3515	224.7	0.2807	0.37
RE(1)X	2.2865	193.4	0.2416	0.32
RE(2)X	2.2850	192.8	0.2406	0.31
RE(3)X	2.2755	186.6	0.2331	0.30
RE(4)X	2.2520	178.6	0.2231	0.29
$RENH_4X$	2.2590	181.6	0.2269	0.30
NaY	2.3660	232.3	0.2802	0.36
$RENH_4(2)Y$	2.3310	214.3	0.2677	0.33
REY	2.2970	198.2	0.2476	0.31
$RENH_4(1)Y$	2.2950	197.2	0.2463	0.30

This is in close agreement with the value reported by Breck and Grose[69] and others[70]. Similarly the void volumes of NaY (0.35 cm^3/g) calculated from nitrogen adsorption is also in close agreement with the value reported in the literature[70].

The values of void volume in both X and Y type zeolites exchanged with rare-earth and hydrogen plus rare-earth ions (Table-10) indicate that the void volume decreases with increase in the rare-earth content in the zeolite. But partial exchange with hydrogen ions appears to be operative in increasing void volume as may be seen from the comparison of the void volume data for $RENH_4$(2)Y and $RENH_4$(1)Y.

The above results clearly indicate that the cavities in the X and Y type zeolites are modified by the presence of rare-earth and hydrogen ions resulting in the decrease of the void volume, which in turn reduces the sorption capacity as reported by Tsitsishvili[63].

KINETICS OF ADSORPTION OF WATER AND ORGANIC SOLVENTS :

Water forms hydration complex with exchangeable cations and interacts electrostatically with framework oxygen. The hydration complex with monovalent cations is weak and relatively easy. The higher the valence of the cation the stronger is the hydration complex. The nature of the adsorbent surface and adsorbate-adsorbent interaction may be determined from the study of sorption equilibria and various thermodynamic parameters which accompany the sorption process[18].

The sorption kinetics of water vapour on type X and Y zeolites have been measured at 25°C and shown in Figures 11 and 13 respectively. It is seen that the rate as well as the equilibrium sorption values decrease on replacement of Na^+ ions with RE^{3+} or RE^{3+} and H^+ ions in NaX as well as NaY zeolites. The equilibrium values of sorption follow the sequence NaX > RE(1)X > RE(2)X $RENH_4X$ > RE(4)X and NaY > $RENH_4$(2)Y > REY > $RENH_4$(1)Y respectively. The order of the magnitude of the sorption of water in various zeolites is similar to that for nitrogen and may be related to the void volume of the zeolite before and after exchange.

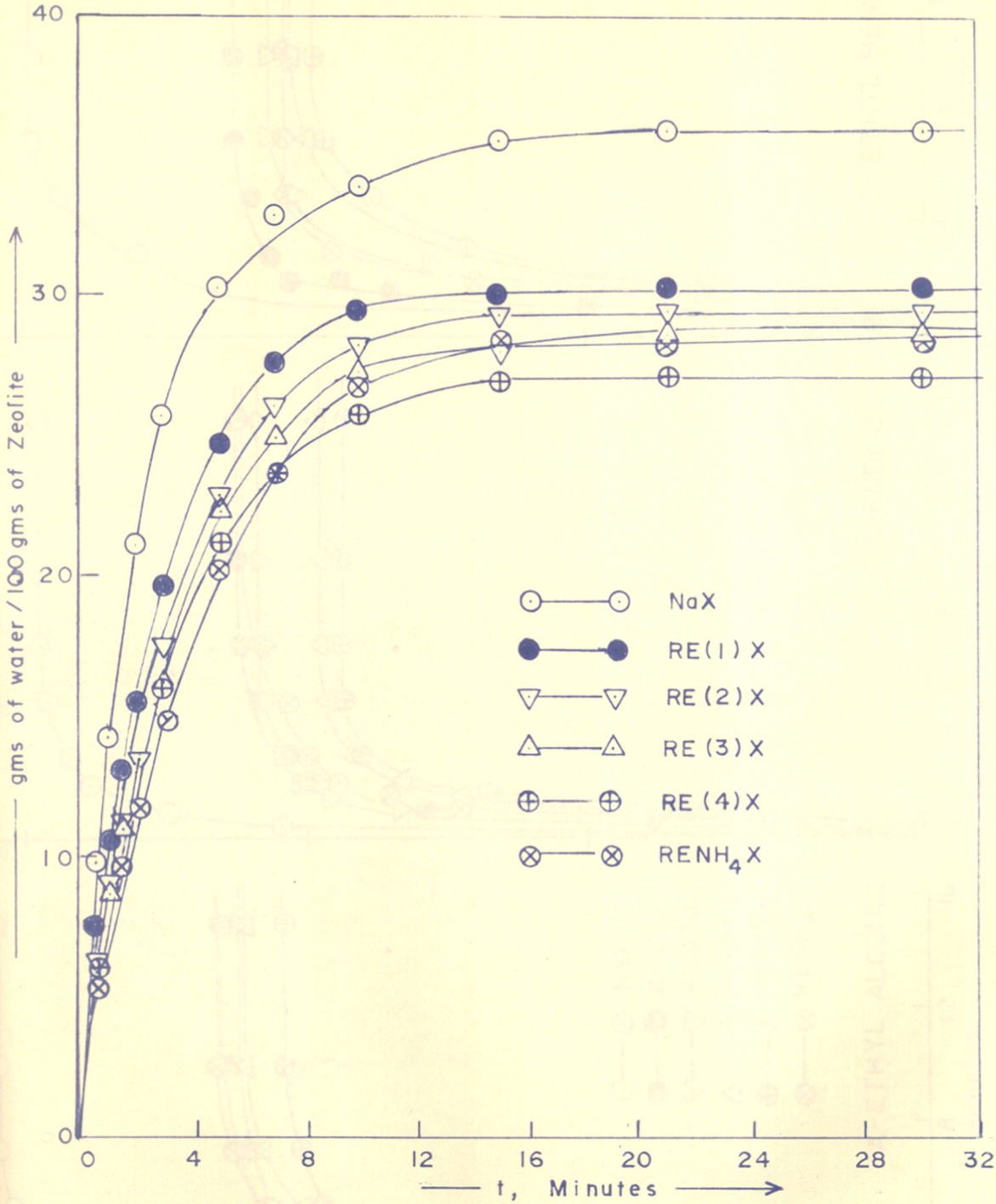

FIG.11. RATE OF ADSORPTION OF WATER VAPOUR ON X TYPE ZEOLITES

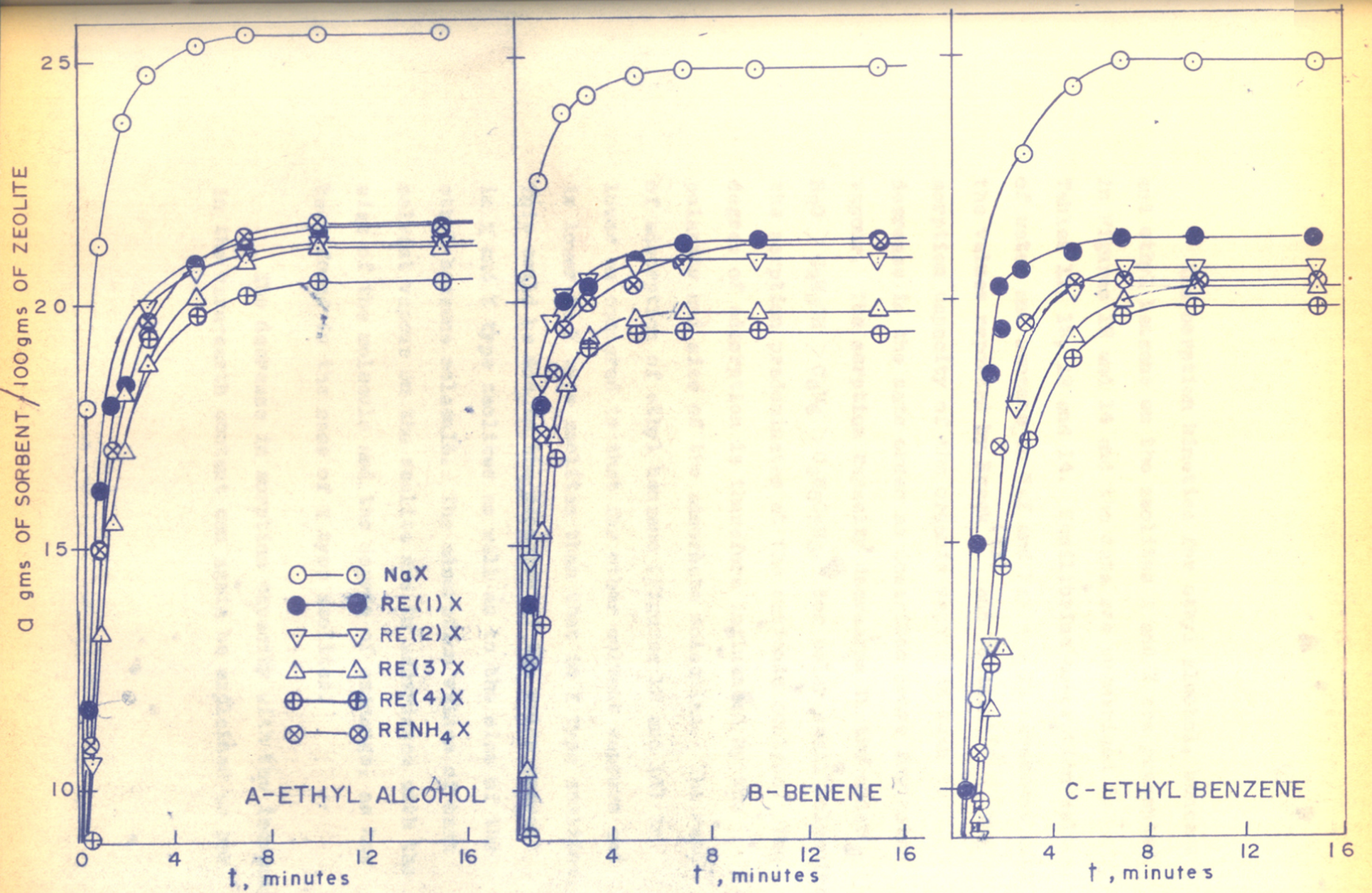

FIG. 12. RATE OF ADSORPTION OF VAPOURS OF A, B & C ON X TYPE ZEOLITES

The sorption kinetics for ethyl alcohol, benzene and ethyl benzene on the zeolites X and Y are presented in Figures 12 and 14 and the data are summarized in Tables 11, 12, 13 and 14. Equilibrium adsorption values of water and benzene in NaY and NaX are in agreement with the values reported by Breck[71] and Dubinin[72]. The sorption capacity of the organic vapour is seen to decrease in the same order as described above for water vapour. The sorption capacity decreases in the order $H_2O > C_2H_5OH > C_6H_6 > C_6H_5C_2H_5$. For polar small molecules the sorption predominates at the cationic centres. The degree of adsorption is therefore influenced by the polarity and size of the adsorbate molecules. The rate of adsorption of ethyl benzene (Figures 12 and 14) is lower as compared to that for other solvent vapours and is lower in Y type zeolites than that in X type zeolites. This could be due to the geometry of the voids present in X and Y type zeolites as well as to the size of the ethyl benzene molecule. The adsorption values of each solvent vapour on the zeolite are in accordance with the size of the molecule and the degree of exchange, as has been found in the case of X type zeolites.

The decrease in sorption capacity with the increase in the rare-earth content can again be explained as per

TABLE-11

SORPTION OF BENZENE AT 25°C (gms./100 gms.)							SORPTION OF ETHYL BENZENE AT 25°C (gms./100 gms.)						
Time in mins.	Zeolite						Time in mins.	Zeolite					
	NaX	RE(1)X	RE(2)X	RE(3)X	RE4(X)	$RENH_4X$		NaX	RE(1)X	RE(2)X	RE(3)X	RE(4)X	$RENH_4X$
1	22.50	17.96	18.42	15.31	13.39	18.46	1	11.67	14.97	9.04	9.38	9.69	10.75
2	23.92	20.06	20.23	18.27	18.52	19.83	2	19.36	20.36	17.76	13.83	14.53	17.08
3	24.32	20.36	20.53	19.26	19.09	20.39	3	23.06	20.66	-	17.04	17.09	20.39
5	24.77	20.96	20.83	19.57	19.38	20.66	5	24.48	20.96	20.36	19.26	18.81	20.66
7	24.77	21.25	20.83	19.75	19.38	20.94	7	24.89	21.26	20.66	20.00	19.66	20.66
10	24.77	21.25	20.83	19.75	19.38	21.22	10	24.89	21.26	20.66	20.25	19.95	-
15	-	-	-	-	-	-	15	-	-	-	-	-	-
20	-	-	-	-	-	-	20	-	-	-	-	-	-
30	-	-	-	-	-	-	30	-	-	-	-	-	-

TABLE-12

Time in mins.	SORPTION OF WATER AT 25°C (gms./100 gms.) Zeolites						Time in mins.	SORPTION OF ETHANOL AT 25°C (gms./100 gms.) Zeolites					
	NaX	RE(1)X	RE(2)X	RE(3)X	RE(4)X	$RENH_4X$		NaX	RE(1)X	RE(2)X	RE(3)X	RE(4)X	$RENH_4X$
1	14.24	10.30	8.94	8.56	7.98	9.92	1	21.35	16.17	14.85	13.33	14.82	16.81
2	21.07	15.39	13.29	13.13	12.25	14.05	2	23.81	18.44	18.40	17.04	18.24	19.29
3	25.63	19.58	17.38	16.28	15.96	18.18	3	24.77	19.52	20.02	18.77	19.38	20.66
5	30.18	24.67	22.75	22.28	21.09	23.14	5	25.46	20.96	20.66	20.24	19.95	21.49
7	32.75	27.66	24.07	24.85	23.65	26.45	7	25.63	21.26	20.99	20.98	20.23	21.77
10	33.89	29.34	28.12	27.12	2565	27.55	10	25.63	21.53	21.31	21.23	20.52	21.77
15	34.45	29.94	29.14	27.99	26.78	28.93	15	-	-	-	-	-	-
20	34.74	30.23	29.39	28.56	27.07	29.20	20	-	-	-	-	-	-
30	-	-	-	28.85	-	29.48	30	-	-	-	-	-	-

TABLE - 13

SORPTION OF BENZENE AT 25°C (gms./100 gms.)					SORPTION OF ETHYL BENZENE AT 25°C (gms./100 gms.)				
Time in mins.	Zeolites				Time in mins.	Zeolites			
	NaY	REY	$RENH_4(2)Y$	$RENH_4(1)Y$		NaY	REY	$RENH_4(2)Y$	$RENH_4(1)Y$
1	24.06	18.52	17.38	17.20	1	9.57	8.55	7.57	8.19
2	25.22	19.75	18.70	19.11	2	13.92	14.53	12.12	12.56
3	25.51	20.35	19.75	19.65	3	18.97	17.38	15.15	16.38
5	25.80	20.92	20.54	20.20	5	22.61	19.66	20.00	19.10
7	26.09	21.09	21.06	20.47	7	24.35	20.52	21.82	19.92
10	26.09	21.09	21.33	20.47	10	24.64	20.80	23.04	20.20
15	-	-	21.59	-	15	24.64	20.80	23.04	20.20
20	-	-	21.59	-	20	-	-	-	-
25	-	-	-	-	25	-	-	-	-
30	-	-	-	-	30	-	-	-	-

TABLE - 14

SORPTION OF WATER AT 25°C (gms./100 gms.)					SORPTION OF ETHANOL AT 25°C (gms./100 gms.)				
Time in mins.	Zeolites				Time in mins.	Zeolites			
	NaY	REY	$RENH_4(2)Y$	$RENH_4(1)Y$		NaY	REY	$RENH_4(2)Y$	$RENH_4(1)Y$
1	11.01	7.40	7.11	7.92	1	20.58	16.81	16.06	16.38
2	16.52	10.83	11.32	11.46	2	23.19	20.23	19.75	20.20
3	20.00	14.25	14.22	15.01	3	24.06	21.94	21.33	21.29
5	24.93	19.66	19.49	19.38	5	24.93	23.08	22.12	22.38
7	27.83	23.37	23.70	23.75	7	25.22	23.37	22.91	22.65
10	29.57	27.36	27.39	26.75	10	25.22	-	23.17	22.65
15	30.73	29.06	29.23	28.38	15	-	-	23.17	-
20	-	29.35	29.23	28.93	20	-	-	-	-
25	31.02	29.35	-	28.93	25	-	-	-	-
30	31.02	29.35	-	-	30	-	-	-	-

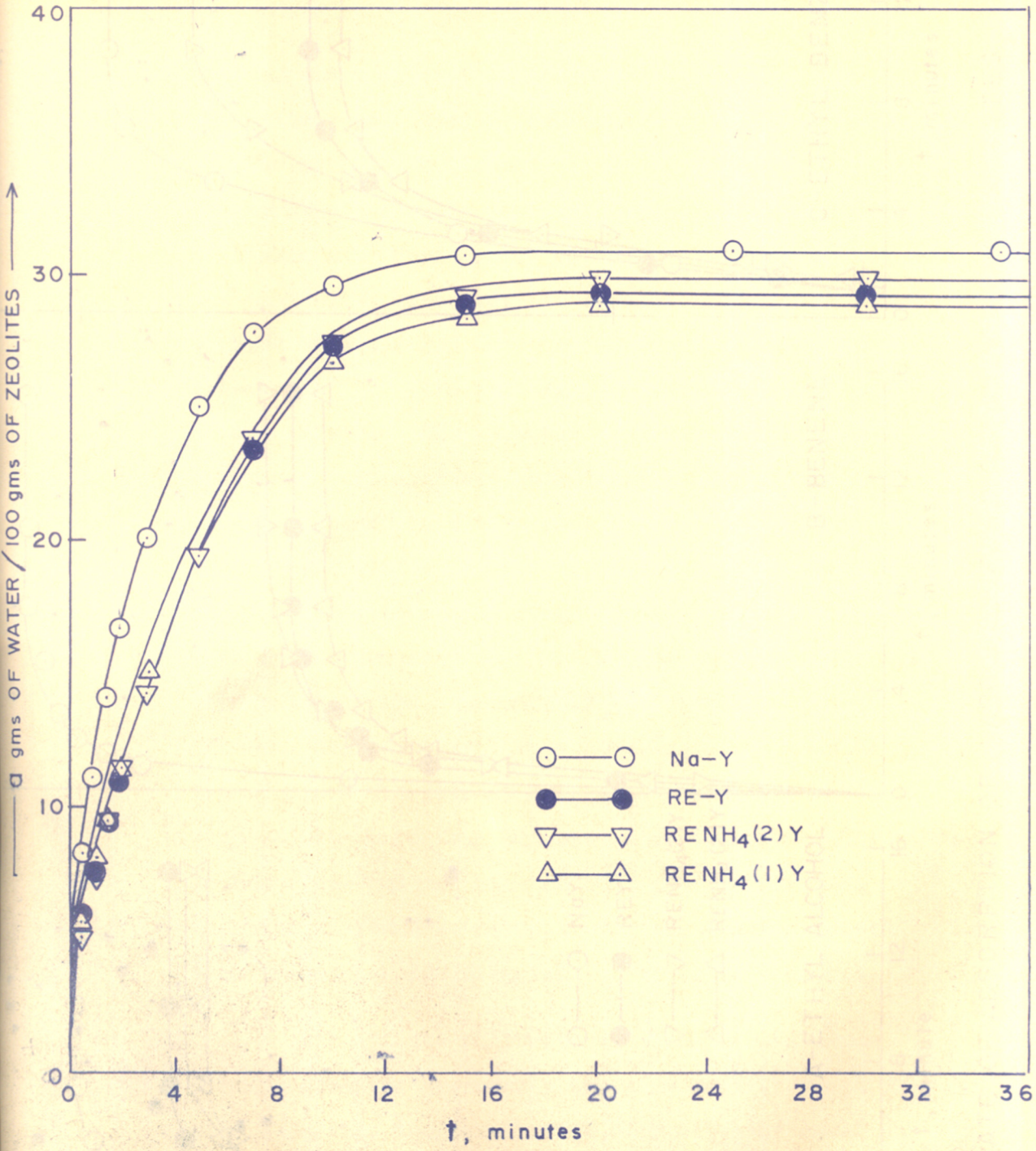

FIG. 13. RATE OF ADSORPTION OF WATER VAPOUR ON Y TYPE ZEOLITES

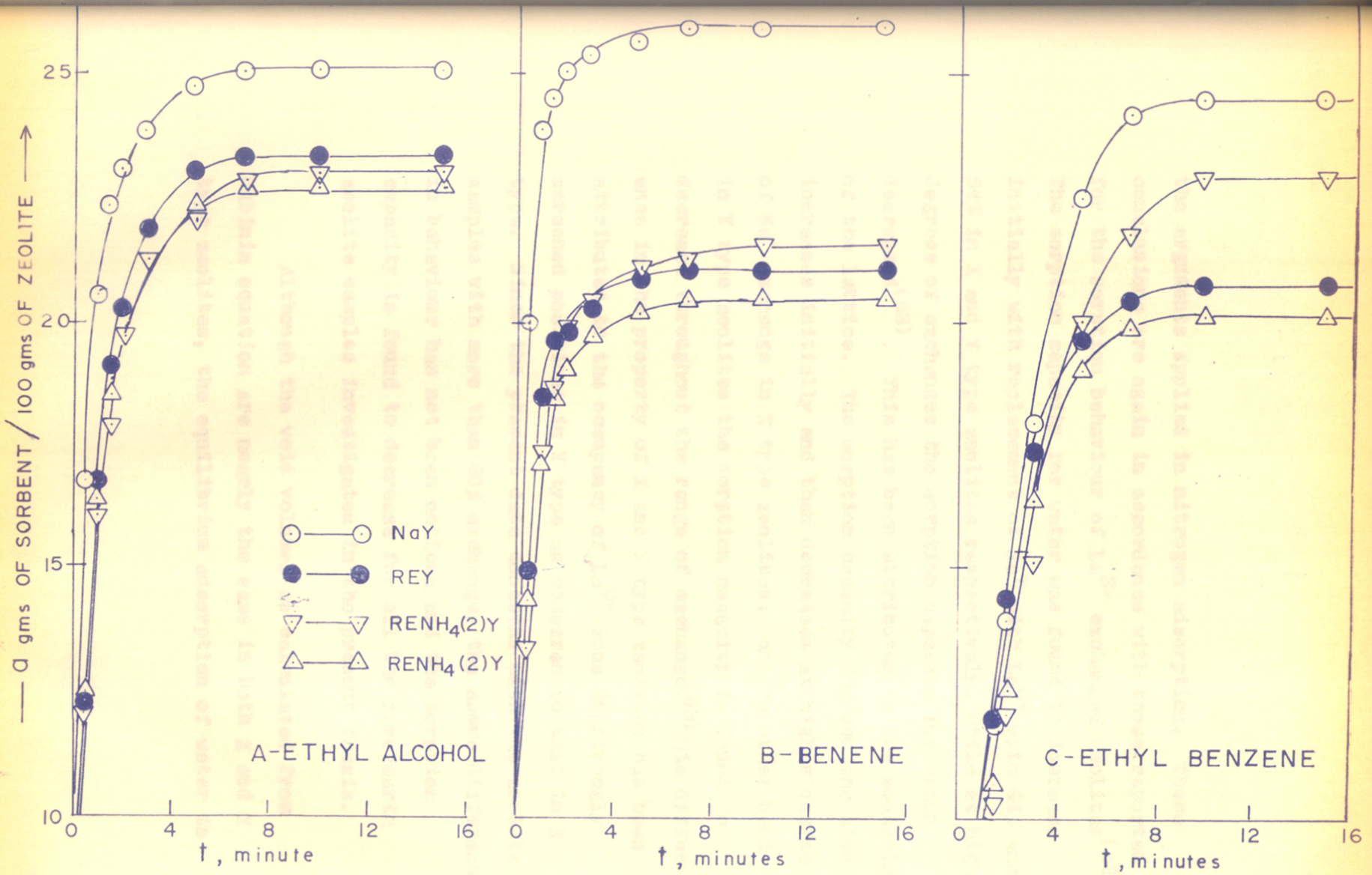

FIG.14. RATE OF ADSORPTION OF VAPOURS OF A, B & C ON Y TYPE ZEOLITES

the arguments applied in nitrogen adsorption. These conclusions are again in accordance with those reported for the sorption behaviour of La^{3+} exchanged zeolites[63]. The sorption capacity for water was found to increase initially with replacement of Na^{+} with La^{3+} upto 44% and 64% in X and Y type zeolites respectively, while at higher degrees of exchanges the sorption capacity for water decreased[63]. This has been attributed to the weakening of the lattice. The sorption capacity for benzene also increases initially and then decreases at higher degree of Na^{+} exchange in X type zeolites; on the other hand in Y type zeolites the sorption capacity is found to decrease throughout the range of exchange.[63] This difference in the property of X and Y type zeolites has been attributed to the occupancy of La^{3+} ions in strongly screened positions in Y type as compared to that in X type. Since the present data concerns with the zeolite samples with more than 80% exchange, the above difference in behaviour has not been noticed and the sorption capacity is found to decrease for all the rare-earth zeolite samples investigated in the present thesis.

Although the void volumes as calculated from Dubinin equation are nearly the same in both X and Y type zeolites, the equilibrium adsorption of water is

considerably lower in Y type zeolites than in X type; on the other hand the adsorption of nitrogen (at 78°K) is considerably higher in Y type zeolites than in X type zeolites. The study of adsorption of water vapour on Ca or Sr zeolites indicate[63A] that the replacement of Na^{+} by Ca^{2+} or Sr^{2+} also decreased the degree of adsorption. Such a behaviour is probably due to the fact that Ca^{2+} (Sr^{2+}) ions occupy S_I and S_{II} sites in the exchange process and the number of the cationic centres per unit cell diminishes. The adsorption capacity is also influenced by the formation of OH groups. Trivalent RE^{3+} ions in zeolite X and Y interact strongly with polar water molecules even at comparatively screened positions.

DIFFUSION COEFFICIENT :

Diffusion in porous pellets is often the rate limiting process in industrial adsorption or catalytic processes. Intracrystalline diffusion process can be represented by Fick's law. For the two component system of sorbate and zeolite, Barrer[73] has defined five different types of diffusion coefficients. The inter-diffusion coefficient D_{AB} or simply diffusion coefficient D is most common and can be calculated from the measurement of the rate of sorption at constant pressure. Therefore, the diffusion coefficient may be evaluated using the following relation[73] :

$$\frac{Q_t - Q_o}{Q_\infty - Q_t} = \frac{2A}{V} \cdot (Dt/\pi)^{\sqrt{2}} \qquad \ldots\ldots (13)$$

where Q_t, Q_o and Q_∞ are amounts of the sorbates adsorbed at time 't', 'zero' and at equilibrium (∞) respectively, V is the volume of the zeolite powder and A is the external surface area of the zeolite and D is the diffusion coefficient. The volume V of the Zeolite is determined from the density of the zeolite in the hydrated form. The density of the hydrated zeolite is given by

$$d = \frac{1.66}{V} \cdot \frac{(M)}{} = \frac{1.66(59x + 60y)}{V^*}$$

$\ldots\ldots$ (14)

where M is the formula weight of the framework of the zeolite, x and y are the number of (AlO_2) and (SiO_2) per unit cell and V* is the unit cell volume in $\mathring{A}^3$.

The total external surface area (A) is determined in several ways. For example, it may be determined from the adsorption of N_2 or Kr_2 on water-filled crystals, so that N_2 or Kr_2 sorption is limited to the external surface only. Barrer and Brook[74], on the other hand, suggested a simple method for determining the external surface area from the relation

$$Q_t - Q_o = Ak\,t^{\frac{1}{2}} + \Delta \qquad \ldots\ldots (15)$$

where 'Δ' corresponds to a nearly monolayer adsorption and is obtained from foot of the plot of (Q_t-Q_o) against $t^{\frac{1}{2}}$. Knowing the area of the sorbate molecule the external surface area may therefore be evaluated. The diffusion coefficient D is then evaluated from the plot of $(Q_t-Q_o)/(Q_\infty-Q_o)$ against $t^{\frac{1}{2}}$. The slope (s) of the straight line portion of this graph is then $(2A/V).(D/\pi)^{\frac{1}{2}}$. By knowing A and V*, the diffusion coefficient is then calculated using the relation

$$D = \frac{s^2 V^2 \pi}{4A^2} \qquad \ldots\ldots (16)$$

For determining the external surface area of the different X and Y type zeolites, the value of V is evaluated by taking density of the zeolite to be 1.27 cm^3/g.[75] The external surface area is computed by using sorption measurements with water as sorbate and taking its molecular area as 10.6 $\mathring{A}^2$ [76]. The external surface area is estimated to be $\sim$14 m^2/g. This value is somewhat higher than the values reported by Venuto et al.[77] However, within the limits of experimental error this value of external area was assumed to be constant for different faujasites.

The Table-15 summarizes the values of diffusion coefficient (D) at 25°C for different zeolites. The diffusion coefficient D calculated for water is 4.52 x 10^{-12} cms/sec. and is in general agreement with the values reported in literature[74,78] for other sorbates on different zeolites.

In general the diffusion coefficient for water is found to decrease with the increase in sodium replacement; on the other hand with other sorbates studied 'D' is found to increase with the increase in sodium replacement. The diffusion coefficient is found to be higher for ethyl benzene than for other sorbates. This may be attributed to the larger size of the ethyl benzene as compared to

TABLE-15 : DIFFUSION OF SORBATES IN ZEOLITES

Zeolite	Diffusion coefficient (D) x 10^{12}			
	H_2O	C_2H_5OH	C_6H_6	$C_2H_5.C_6H_5$
NaX	4.52	2.46	1.73	13.59
RE(1)X	3.45	7.95	2.97	12.82
RE(2)X	3.12	7.95	5.13	16.93
RE(3)X	2.79	6.92	12.21	12.31
RE(4)X	2.79	4.51	15.90	8.98
$RENH_4X$	3.02	6.40	7.95	12.31
NaY	3.02	3.08	6.92	4.62
REY	2.55	7.95	7.69	9.75
$RENH_4(2)Y$	2.28	5.39	5.90	5.90
$RENH_4(1)Y$	2.50	5.39	4.10	6.92

other sorbate molecules. A decrease in the value of diffusion coefficient is also reported by Tsitsishvili et al.[63] passing from Na-A zeolite to CsA with water as adsorbate. This indicates that number, size, valence and location of cations in the lattice of the zeolite influence the value of diffusion coefficient. The data tabulated in Table-15 indicate that dimension and polarity of adsorbate molecules also influence diffusion coefficient.

THERMAL ANALYSIS AND STABILITY OF ZEOLITES :

The thermal stability of ion exchanged zeolites may be evaluated from the variation in (a) X-ray, i.r. patterns, (b) sorption capacity or (c) shift in the positions of the exothermic peak in the DTA curve. In the following the thermal stability of rare-earth zeolites is determined from the thermal analysis.

The TGA curves for the type X zeolites are shown in Figure 15. The dehydration starts at about 40-60°C and is complete at about 450°C. The rate of dehydration depends on the concentration and the type of the cation. The weight loss occurs slowly and over a relatively larger temperature range as the degree of exchange increases. The loss in weight decreases with the increase in the degree of exchange (Table-16). This may be a consequence of the decrease in the sorption capacity with the degree of exchange as discussed earlier under sorption properties.

The DTA curves for X type zeolites are shown in Figure-16. The low temperature endothermic and high temperature exothermic peaks are markedly seen in the figure. A comparison of DTA and TGA curves shows that the endothermic peak corresponds to the liberation of water from the zeolite. From the figure 16 and table-16

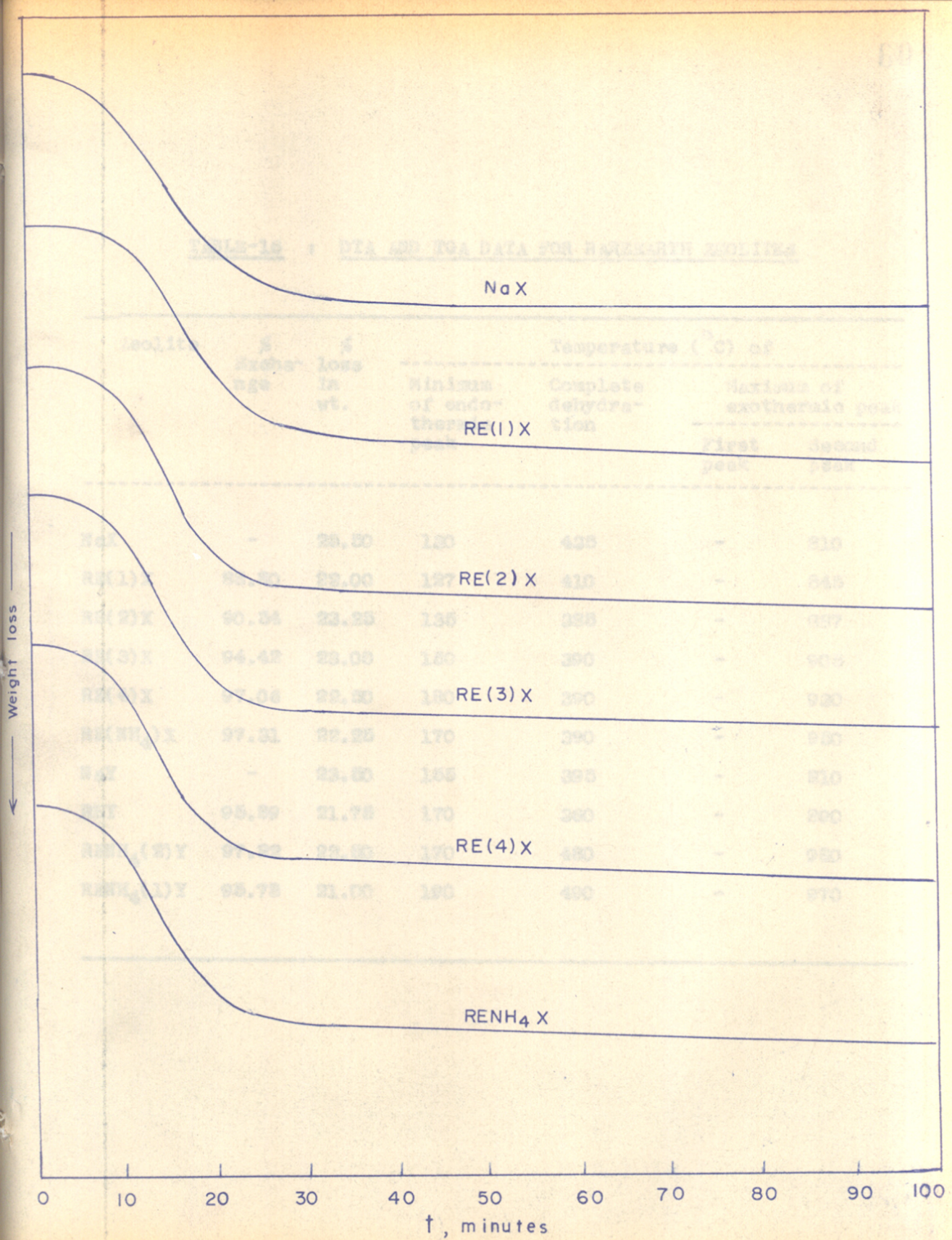

FIG.15. TGA OF X-TYPE ZEOLITES

TABLE-16 : DTA AND TGA DATA FOR RAREEARTH ZEOLITES

Zeolite	% Exchange	% loss in wt.	Temperature (^{o}C) of			
			Minimum of endothermic peak	Complete dehydration	Maximum of exothermic peak	
					First peak	Second peak
NaX	-	25.50	130	435	-	810
RE(1)X	88.80	22.00	127	410	-	845
RE(2)X	90.54	23.25	135	385	-	887
RE(3)X	94.42	23.00	150	390	-	905
RE(4)X	97.06	22.50	180	390	-	930
RE(NH_4)X	97.31	22.25	170	390	-	950
NaY	-	23.50	155	395	-	810
REY	95.89	21.75	170	360	-	890
RENH_4(2)Y	97.22	22.50	170	480	-	980
RENH_4(1)Y	95.78	21.00	190	490	-	970

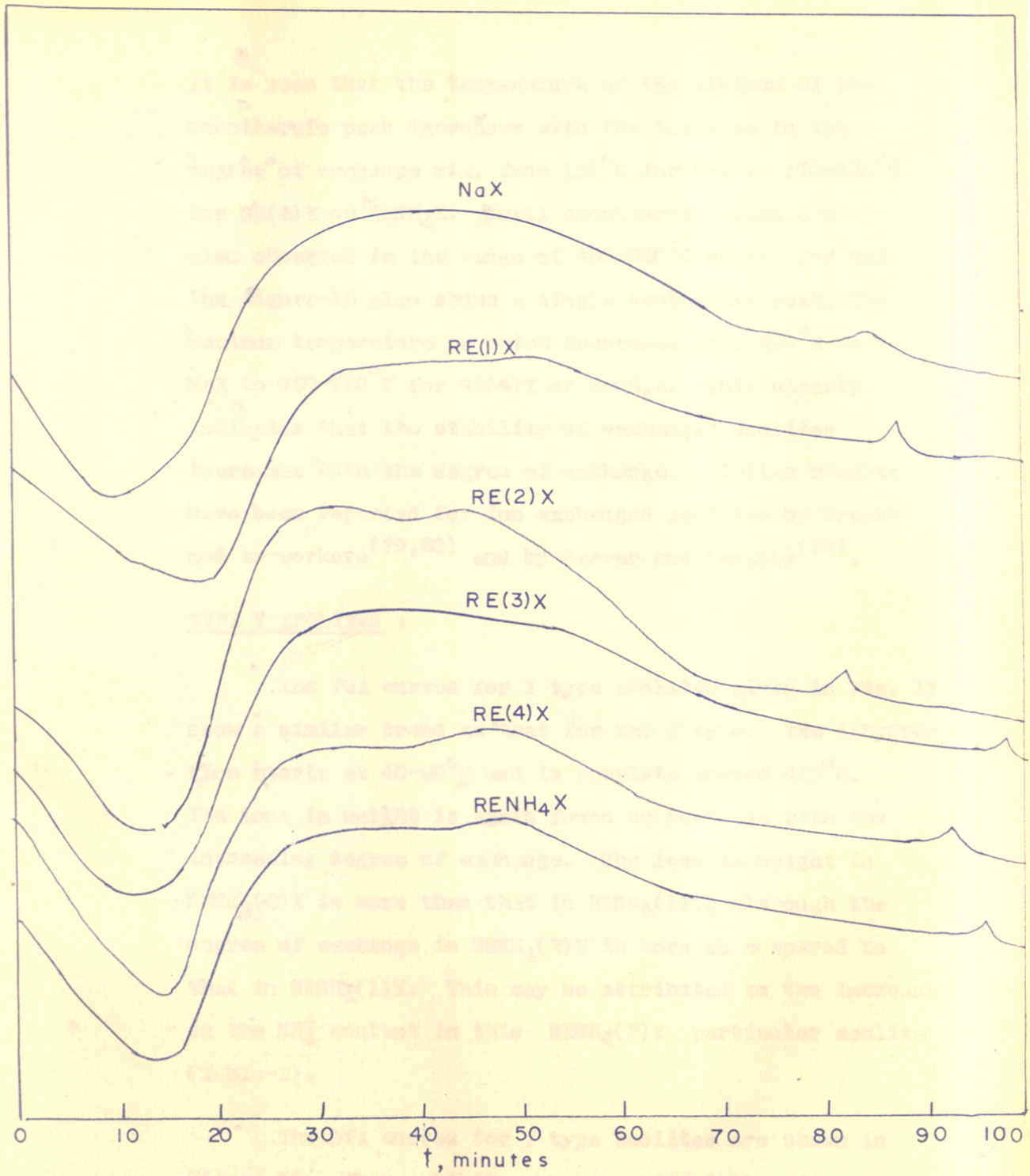

FIG.16. DTA OF X TYPE ZEOLITES

it is seen that the temperature of the minimum of the endothermic peak increases with the increase in the degree of exchange viz. from 130°C for NaX to 170-180°C for RE(4)X or $RENH_4X$. Small endothermic peaks are also observed in the range of 480-550°C except for NaX. The Figure-16 also shows a single exothermic peak, the maximum temperature of which increases from 810°C for NaX to 930-950°C for RE(4)X or $RENH_4X$. This clearly indicates that the stability of exchanged zeolites increases with the degree of exchange. Similar results have been reported for ion exchanged zeolites by Bremer and co-workers[79,80] and by Barrer and Langley[29].

TYPE Y ZEOLITES :

The TGA curves for Y type zeolites given in Fig. 17 show a similar trend as that for the X type. The dehydration starts at 40-60°C and is complete around 410°C. The loss in weight is again found to decrease with the increasing degree of exchange. The loss in weight in $RENH_4(2)Y$ is more than that in $RENH_4(1)Y$, although the degree of exchange in $RENH_4(2)Y$ is more as compared to that in $RENH_4(1)Y$. This may be attributed to the increase in the NH_4^+ content in this $RENH_4(2)Y$ particular zeolite (Table-3).

The DTA curves for Y type zeolites are shown in Figure 18. They exhibit a pronounced endothermic peak.

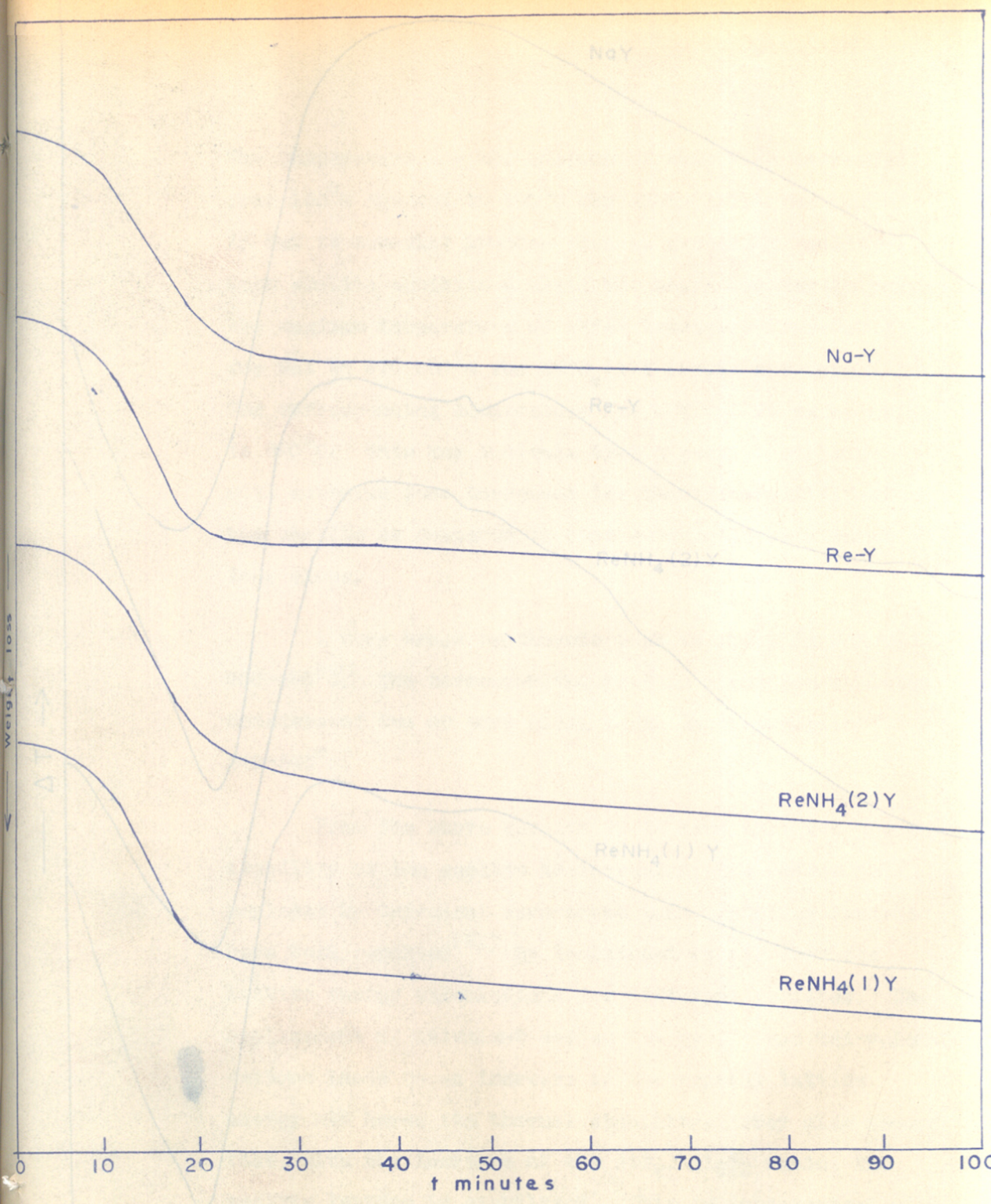

FIG.17. TGA OF Y TYPE ZEOLITES

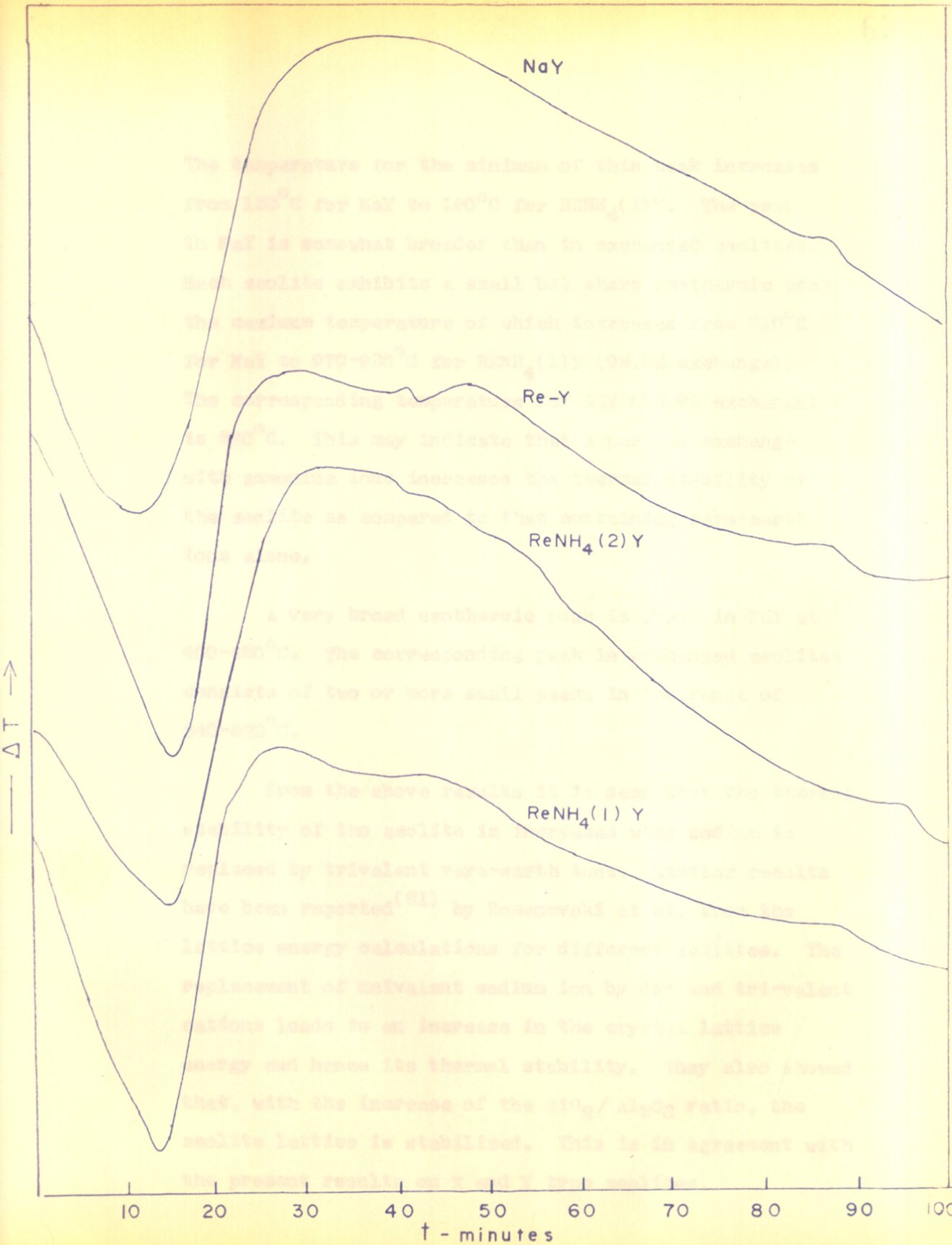

FIG. 18. DTA OF Y TYPE ZEOLITES

The temperature for the minimum of this peak increases from 155°C for NaY to 190°C for $RENH_4$(1)Y. The peak in NaY is somewhat broader than in exchanged zeolites. Each zeolite exhibits a small but sharp exothermic peak, the maximum temperature of which increases from 810°C for NaY to 970-980°C for $RENH_4$(1)Y (95.8% exchange). The corresponding temperature for REY (95.9% exchange) is 890°C. This may indicate that a partial exchange with ammonium ions increases the thermal stability of the zeolite as compared to that containing rare-earth ions alone.

A very broad exothermic peak is found in NaY at 400-480°C. The corresponding peak in exchanged zeolites consists of two or more small peaks in the range of 340-520°C.

From the above results it is seen that the thermal stability of the zeolite is increased when sodium is replaced by trivalent rare-earth ions. Similar results have been reported[81] by Romanovski et al. from the lattice energy calculations for different zeolites. The replacement of univalent sodium ion by di- and tri-valent cations leads to an increase in the crystal lattice energy and hence its thermal stability. They also showed that, with the increase of the SiO_2/Al_2O_3 ratio, the zeolite lattice is stabilized. This is in agreement with the present results on X and Y type zeolites.

ACTIVATION ENERGY FOR DEHYDRATION :

From the kinetic equation for the rate of dehydration, Piloyan and Novikova[82] obtained the following relationship.

$$\frac{1-(1-\alpha)^{1-n}}{1-n} = \frac{ART^2}{E.b} \cdot e^{-E/RT} \qquad \ldots\ldots (17)$$

where m is the weight loss at time t and μ is the total weight loss, $\alpha = m/\mu$, the relative weight loss, n is the order of reaction, T is the temperature in degrees Kelvin and R is the molar gas constant. 'A' is frequency factor and 'b' is the rate of heating of the sample. The equation (17) after simplification takes the form

$$\ln (m/T^2) = A' - \frac{E_{TG}}{RT} \qquad \ldots\ldots (18)$$

The energy of activation E_{TG} is equal to the 2.303 RT.S where 'S' is the slope of the plot of log (m/T^2) against 1/T. Similarly Coats and Redfern[83] obtained the following relation from kinetic considerations :

$$\log_{10}\left[\frac{-\log_{10}(1-\alpha)}{T^2}\right] = \log \frac{A.R}{E.b}\left(1 - \frac{2RT}{E}\right) - \frac{E}{2.303\ RT}$$

$\ldots\ldots$ (19)

The activation energy is therefore obtained as 2.303 RT.S where 'S' is the slope of the linear plot of log $\left[\frac{-\log(1-\alpha)}{T^2}\right]$ against 1/T.

The activation energy E_{DTA} may be obtained by using the relation[82]

$$\ln \Delta t = C' - \frac{E_{DTA}}{RT} \quad \ldots\ldots (20)$$

where Δt is the deviation of the DTA curve from the base line.

The energy of activation has been calculated from slopes of the linear plots using equations (18) and (20) in the range of 80-120°C and the equation (19) in the range of 90-240°C. The order of reaction is evaluated separately by using "shape Index" factor 'S' for the endothermic peak in DTA curve using the relation[84]

$$n = 1.26 / \sqrt{S} \quad \ldots\ldots (21)$$

The values of 'n' and the activation energies obtained for different zeolites are summarized in Table-17. It is clear that the dehydration of the zeolite follows first order kinetics ($n = 0.9 \pm 0.15$). This is in agreement with the literature[85,86]. The values of activation energies from the three methods discussed above agree within the limits of experimental error. The activation energies obtained for NaX and NaY are comparable with the reported[86] values. The activation energies for different zeolites range between 4-7 Kcals/mole. The activation energies are somewhat lower for the zeolite containing H^+ ions.

TABLE-17 : ACTIVATION ENERGY (Kcals/deg.mol.) FOR DEHYDRATION OF ZEOLITES

Zeolite	E	E_{TGA}	E_{DTA}	n
NaX	4.61	4.51	3.88	1.05
RE(1)X	6.61	6.82	6.89	0.74
RE(2)X	4.21	4.86	4.94	0.86
RE(3)X	5.47	5.47	5.47	0.85
RE(4)X	5.16	5.59	5.39	0.97
RE(NH_4)X	5.03	5.14	5.18	0.89
NaY	5.95	5.61	5.51	1.01
REY	6.79	6.66	6.20	0.80
RENH_4(2)Y	6.07	5.96	6.17	0.79
RENH_4(1)Y	4.88	5.19	5.24	0.96

INFRARED SPECTRA :

The X and Y type faujasites having most open framework structures, possess distinct spectral characteristics[89]. The i.r. spectra of different X and Y type zeolites are shown in Figures 19 and 20 respectively. Spectra for NaX and NaY are in agreement with the literature[87,88]. NaX gives absorption bands at 345, 328, 367, 408, 460, 559, 667 and 690 cm^{-1}. The assignment of various bands are given in Table-18. The absorption frequencies and intensities of the bands summarized in Table-18 are in accordance with Flanigen's assignment[89].

The spectra of X type zeolites show major changes when the sodium is replaced with the rare-earth and hydrogen ions. The intensity of the bands at 667, 559 and at 460 cm^{-1} diminishes progressively with the increase in the degree of exchange. The bands at 367 and 408 cm^{-1} are absent in RE(3)X and RE(4)X zeolites but are present in $RENH_4X$ with very low intensity. The intensities of the structure sensitive bands at 780, 570 and 380 cm^{-1} decrease proportionally to the decrease in X-ray intensities of the lines.

The absorption bands in NaY lie at 328, 380, 453 and 578 cm^{-1}. In rare-earth exchanged Y type zeolites, the intensity of the bands at 576, 458 and 380 cm^{-1}

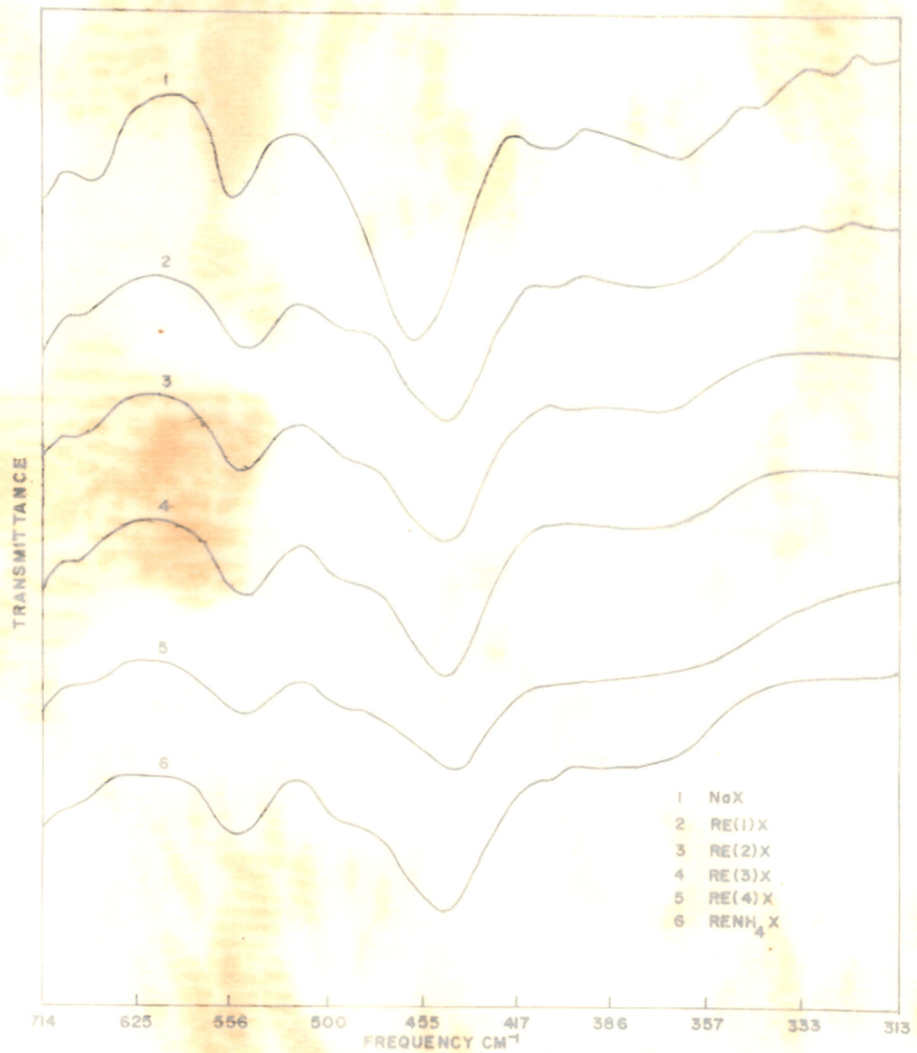

FIG INFRA RED SPECTRA OF X TYPE ZEOLITES (RE & NH_4 EXCHANGED)

Fig. 19 : INFRARED SPECTRA OF X TYPE ZEOLITES

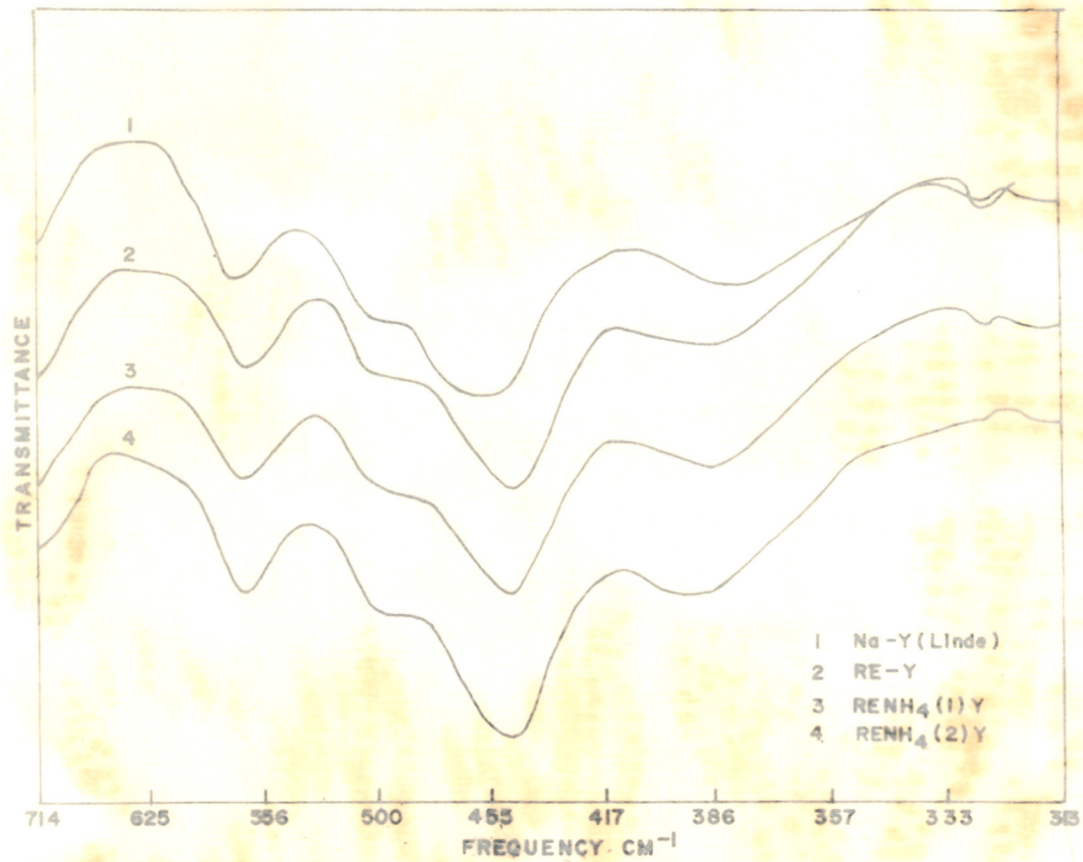

FIG INFRA RED SPECTRA OF Y TYPE ZEOLITE (RE & NH_4 EXCHANGED)

Fig. 20 : INFRA RED SPECTRA OF Y TYPE ZEOLITES

TABLE-18 : INFRARED SPECTRAL DATA FOR X AND Y TYPE ZEOLITES

Zeolite	Symmetric stretch	Double rings	T-O bend	Pore openings			
NaX	667 W	559 M	460 MS	408 W	367 BW	345 W	328 W
RE(1)X	677 VW	553 BM (490 VWSH)	445 BMS	404 VW	367 BW	339 BVW	328 BVW
RE(2)X	677 VW	553 BM (485 VWSH)	443 BMS	397 VW	367 BW	-	-
RE(3)X	677 VW	550 BM (485 VWSH)	441 BMS	-	364 BW	-	-
RE(4)X	667 BVW	550 BM (485 VWSH)	438 BMS	-	361 BVW	-	-
$RENH_4X$	675 BVW	553 BM (485 VWSH)	443 BMS	404 VW	366 BW	-	-
NaY	-	578 M (495 VWSH)	453 BMS	380 BW	-	-	328 W
REY	-	568 M (490 VWSH)	446 MS	388 BW	-	-	329 W
$RENH_4(2)Y$	-	568 M (490 VWSH)	446 MS	391 BW	-	-	328 W
$RENH_4(1)Y$	-	564 M (490 VWSH)	446 MS	393 BW	-	-	328 W

V - Very
S - Strong
W - Weak
M - Medium
B - Broad
SH - Shoulder

increases slowly and bands become more sharp as compared to the rather broad bands present in NaY. On the other hand in $RENH_4(1)Y$ and $RENH_4(2)Y$, the intensities of the band at 328 cm^{-1} diminishes. These observations indicate that there are rather less significant changes in spectra of Y type zeolites as compared to those in X type zeolites. This may indicate that Y type zeolites in rare-earth and hydrogen forms are more stable as compared to the corresponding forms of X type zeolites. This is again in agreement with the observations reported earlier[81].

X-RAY :

The X-ray powder patterns for X and Y type zeolites are shown in Figs. 21 and 22 respectively. The relative intensities and the 'd' values are summarized in Table-19. The data for zeolites NaX and NaY are in agreement with the reported[6] values. The Figures 21, 22 and Table-19 indicate some changes in the intensities of RE(4)X and REY zeolites. The rings corresponding to 220 and 311 planes in RE(4)X and 220 in REY are absent. This may be attributed to the high scattering power of the heavy rare-earth ion as compared to sodium ions present in the original zeolites. The other prominent rings remain unaffected. This shows that the crystalline nature of zeolites is retained even after exchanging Na^+ for RE^{3+} ions.

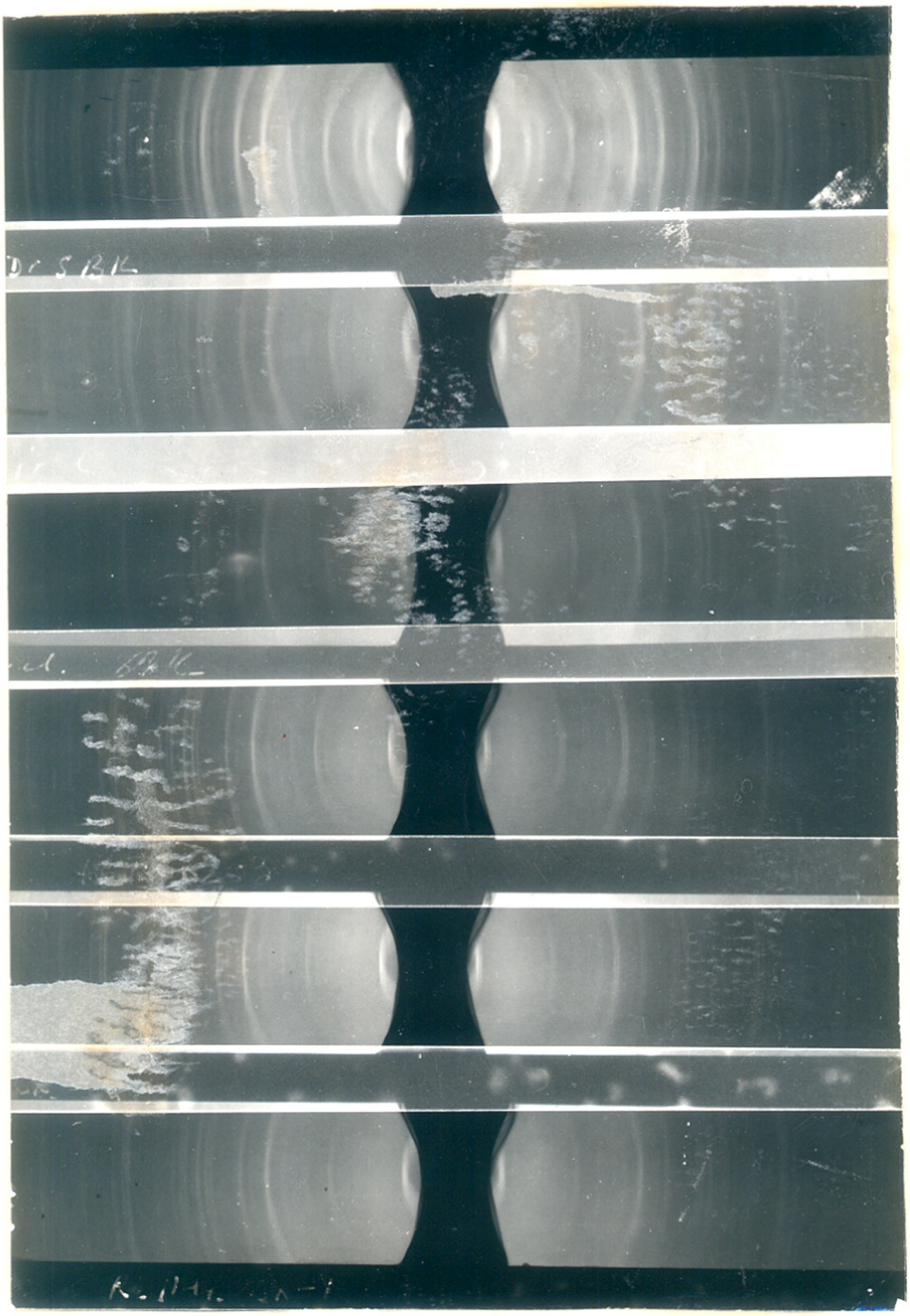

Fig. 21 : X-RAY DIFFRACTION PATTERNS OF X TYPE ZEOLITES

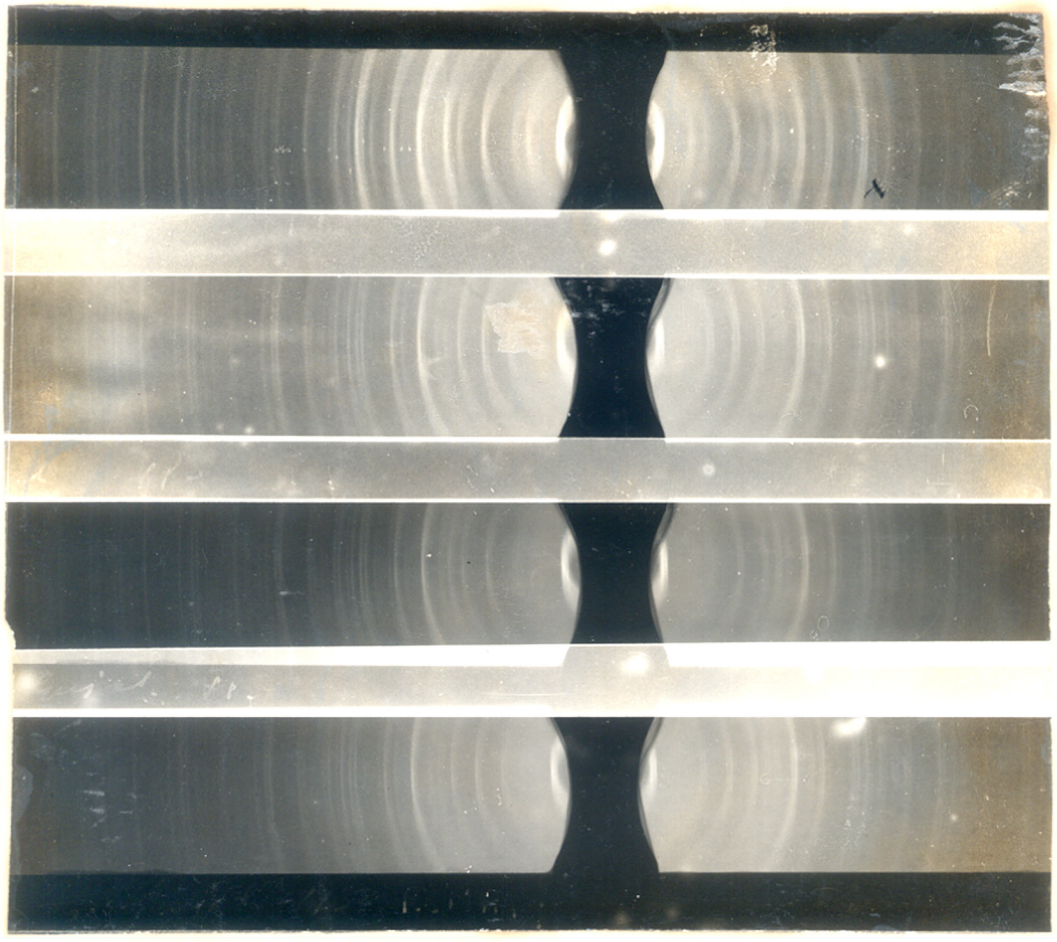

Fig. 22 : X-RAY DIFFRACTION PATTERNS OF Y TYPE ZEOLITES

TABLE-19 : X-RAY POWDER PATTERNS FOR X AND Y TYPE ZEOLITES

X type zeolites					Y type zeolites				
NaX			RE(4)X		NaY			REY	
hkl	d(A)	I	d(A)	I	hkl	d(A)	I	d(A)	I
111	14.34	VS	14.62	VS	111	14.43	VS	14.34	VS
220	8.77	MS	-	-	220	8.73	W	-	-
311	7.43	M	-	-	311	7.46	W	6.91	W
331	5.73	MS	6.16	W	331	5.68	MS	5.74	W
333	4.76	W	4.77	W	333	4.76	W	4.85	W
440	4.39	M	4.38	W	440	4.38	MS	4.32	VW
531	-	-	-	-	620	-	-	-	-
620	4.09	VW	4.13	W	533	3.71	S	3.71	S
533	-	-	-	-	544	3.56	VW	-	-
622	3.77	S	3.77	S	711	3.43	VW	3.42	W
444	-	-	-	-	642	3.28	S	3.26	M
711	3.53	W	3.49	W	731	3.20	VW	-	-

continued.....

TABLE-19 (CONTINUED)

X type zeolites					Y type zeolites				
hkl	d(A)	I	d(A)	I	hkl	d(A)	I	d(A)	I
642	3.31	S	3.31	S	733	3.00	MS	-	-
731	-	-	-	-	822	2.87	W	2.89	M
733	3.04	W	-	-	751	2.84	MS	2.84	M
822	2.92	W	2.93	M	840	-	-	2.74	S
751	2.85	S	2.88	M	911	2.72	VW	2.70	VW
840	2.78	M	2.79	S	644	-	-	-	-
911	-	-	-	-	931	2.61	MS	2.61	MS

VS - Very strong
S - Strong
MS - Medium strong
M - Medium
W - Weak
VW - Very weak

CATALYTIC STUDIES - ALKYLATION :

Synthetic zeolites have been used as catalysts for many reactions. Their catalytic activity depends strongly on the nature of the exchangeable metal cations. Among the various reactions catalysed by ion-exchanged zeolites, alkylation reaction is reported and reviewed by many workers[90-95]. Such reactions generally proceed via carbonium ion type mechanism. Literature[90-95] reveals that zeolites type X and Y, when exchanged with rare-earth, alkaline earth or hydrogen ions, can function as alkylation catalyst.

Vapour-phase alkylation of benzene with ethanol is carried out at 200°C using different rare-earth and hydrogen exchanged X and Y type zeolite catalysts. Although the exact mechanism of the reactions taking place during this alkylation is complex, it may possibly involve the following simple reactions :

$$C_2H_5OH \longrightarrow C_2H_4 + H_2O \quad \ldots\ldots (1)$$

$$C_6H_6 + C_2H_4 \longrightarrow C_6H_5C_2H_5 \quad \ldots\ldots (2)$$

$$C_6H_5.C_2H_5 + C_2H_4 \longrightarrow C_6H_4(C_2H_5)_2 \quad \ldots\ldots (3)$$

$$2C_2H_5OH \longrightarrow (C_2H_5)_2O + H_2O \quad \ldots\ldots (4)$$

Reactions (2) and (3) represent the typical formation of alkylated products along with ethyl benzene. Reaction (4) indicates the possible presence of ether in the product.

The molar ratio of benzene to ethanol in the reaction mixture chosen as 5:1 and liquid hourly space velocity chosen as 10 ml. are in accordance with the unpublished data[96] which indicated maximum conversion of ethanol. The reaction is carried out at 200°C as maximum yield is obtained at this temperature. The alkylated products are analysed by GLC and the activity of the catalyst is estimated in terms of the ethyl benzene formed (conversion of ethanol) in the reaction product at various time intervals.

The results obtained are summarized in Table-20 and are represented in the Figures 23 and 24. The activities follow the sequence $RENH_4X > RE(4)X > RE(3)X > RE(1)X$. The RE(1)X is the least active catalyst and yields 4.25% ethyl benzene at its maximum activity. RE(4)X is more active yielding 8-9% ethyl benzene or 31% conversion (Table-20). It attains maximum activity after 2 hours, then there is a sharp drop in the activity, which remains steady after 6 hours. However, the activity of $RENH_4X$, which shows 63% conversion, is considerably higher as compared to that of RE(4)X. This catalyst also shows a sharp drop in the activity after 5 hours. Figure 23

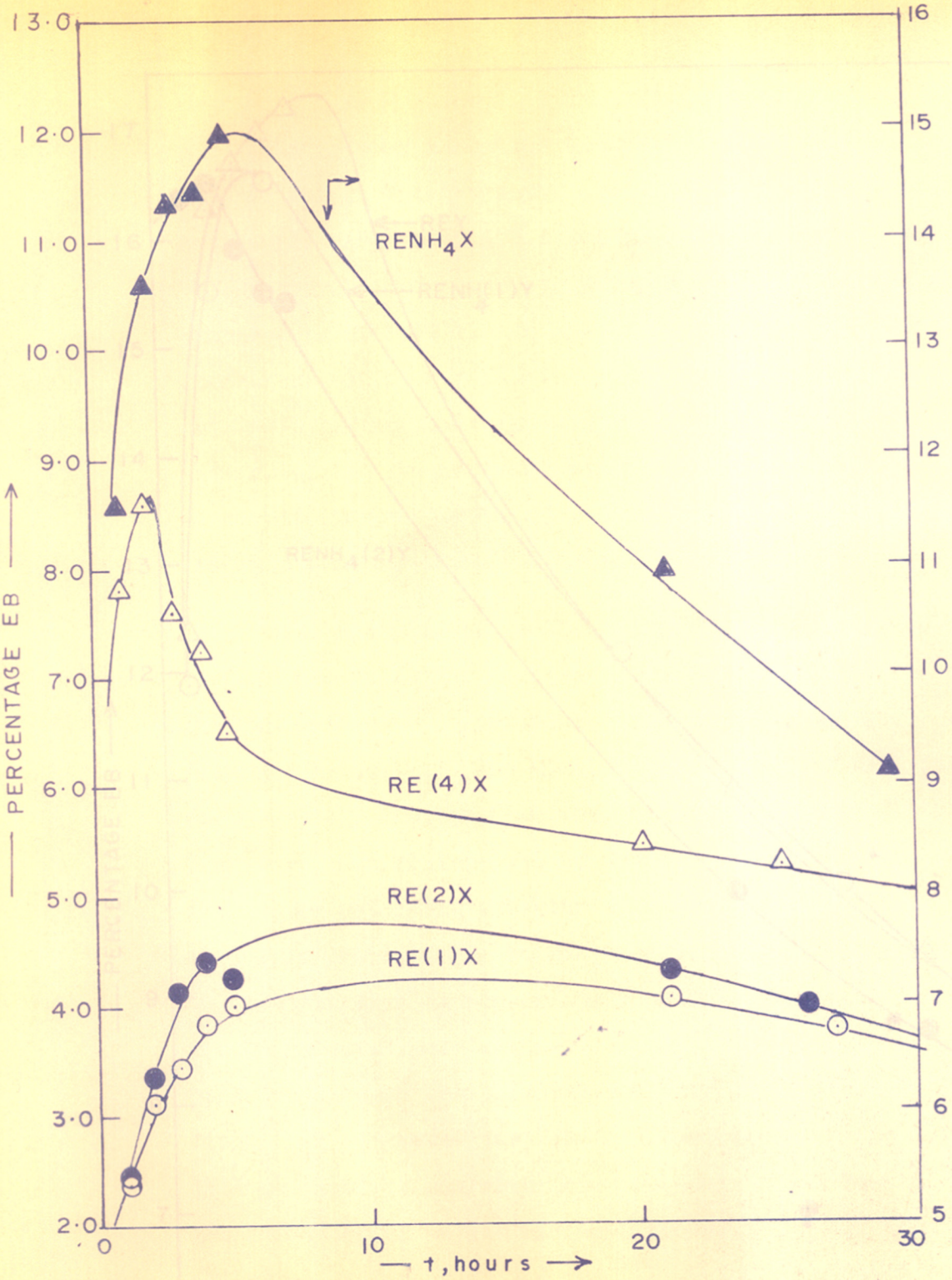

FIG.23. CUMMULATIVE PERCENTAGE ETHYL BENZENE FOR X TYPE CATALYSTS

and Table-20 show a similar change in the activity with time in Y type catalysts. REY and $RENH_4(1)Y$ are equally active yielding about 17% ethyl benzene which corresponds to 72% conversion. However, $RENH_4(2)Y$ is less active as compared to $RENH_4(1)Y$. An appreciable amount of ether (Mechanism 4) is found in the products obtained with catalysts having lower activity while with highly active catalysts, the formation of higher alkyl benzene takes place with longer period of reaction time. This confirms the reaction mechanism (3) indicated above.

The activity of zeolites for carbinogenic reactions is due to strong electrostatic field near the surface cations[97] resulting in a polarization of reactant molecules. The electrostatic field of RE^{3+} ion is remarkably greater than that of Na^+ ions[99]. Therefore, the replacement of sodium with rare-earth introduces catalytic activity in the zeolite and is inversely proportional to the residual sodium content. It is known that carbonium ion type reactions take place due to Brönsted acid centres. Ward[98,99] found a linear relation between the Brönsted activity and electrostatic field. He suggested that field associated with the cation polarizes adsorbed water molecule which results in the formation of acidic hydroxyl group. This has been supported by Turkevich and Ono[100]. The relationship

TABLE-20 : PERCENTAGE YIELD (CONVERSION) WITH TIME FOR DIFFERENT CATALYSTS

Time of reaction (hrs.)	% yield						
	RE(1)X	RE(2)X	RE(4)X	$RENH_4X$	REY	$RENH_4(2)Y$	$RENH_4(1)Y$
1	9.0	9.2	26.5	44.7	41.0	58.0	45.3
2	14.6	16.0	31.1	58.4	72.5	65.9	72.7
3	15.7	16.8	19.0	63.3	65.5	54.8	71.7
4	16.6	20.0	20.0	63.2	63.3	54.4	59.4
5	16.0	15.7	18.8	63.2	66.5	57.5	-
21	14.6	16.1	22.0	36.5	34.7	29.7	41.4
28	10.0	9.8	9.0	16.0	14.6	14.8	18.8

between the catalytic activity and the nature of cations has been discussed by Cross, Kemball and Leach[101] and by Ballivet et al.[102]

All the above arguments lead to conclusion that the catalytic activity is linearly related to Brönsted ~~activity~~ acidity, which in turn is dependent on the degree of sodium replacement. Also cations in S_{II} sites are catalytically more active. The number of cations in S_{II} sites increases with the increase in the degree of exchange. This explains why the catalyst RE(4)X is more active as compared to RE(1)X. The enhanced catalytic activity of $RENH_4X$ over that of RE(4)X with the same residual sodium content may be attributed to the higher activity of cation-decationized zeolites[103,53].

Topchieva et al.[103] showed that the catalytic activity of cation-decationized zeolites depends also on the order of introduction of the active components. The specimens in which trivalent cations are introduced first are more stable and active catalysts as compared to those in which ammonium ion is introduced first and rare-earth ions later. As mentioned earlier in the experimental section, in $RENH_4(2)Y$ catalyst ammonium ion is introduced first while in $RENH_4(1)Y$ the rare-earth ions are introduced first. Therefore, the catalyst $RENH_4(1)Y$ is expected and

is found to be more stable and active as compared to $RENH_4(2)Y$ and is in accordance with the data reported[53,104] earlier.

CATALYTIC DEACTIVATION :

The decrease in the activity or aging of the catalyst is shown in figures 23 and 24 in terms of cummulative percentage of ethyl benzene formed as a function of reaction time. The activity curves in X type catalysts are related to the rare-earth content of the catalyst. In Y type zeolites the activity curve for REY is slightly above that for the $RENH_4(1)Y$, while $RENH_4(2)Y$ has lower activity as compared to $RENH_4(1)Y$. The Y type zeolites are catalytically more active than the corresponding X type zeolites. This has been attributed[105,106] to the higher silica-alumina ratio and larger inter-aluminium distance in Y type zeolites, which leads to higher thermal stability in the catalyst. The transitions from Brönsted to Lewis acid sites is also reversible when silica-alumina ratio is higher.

Figures 23 and 24 also give an insight in the aging (rise and fall in the activity) of the catalyst. In general, it is seen that the catalyst ($RENH_4X$, RE(4)X, $RENH_4(1)Y$ and REY etc.) which are most active indicate faster drop in the activity with time, and the catalysts RE(1)X, RE(3)X which

are relatively less active show slow aging with time.

The fall in the activity of zeolite based catalyst may be due to following causes[107] : (1) Surface reconstitution, (2) Collapse of the crystal structure, and (3) Carbon deposition. In case of hexane cracking and isomerization on decationized Y catalysts, Tung et al.[107] attributed the deactivation of the catalyst to first cause. In the present reaction, the deactivation may be due to carbon deposit. The used catalyst is found to be covered with carbon (black) deposit and when reactivated in presence of oxygen at 450°C, the activity is restored to some extent.

The aging of the catalyst may also be attributed[108] to the polymerization of the ethylene followed by isomerization and cyclodehydrogenation. This process results in the formation of hydrogen-deficient aromatics (coke) within the pores. Since carbonization is accompanied by a decrease in the ion-exchange capacity, it is concluded[109] that the carbon deposits on the catalytically active centres and thus reduces the activity. It is also suggested that with unsaturated compounds, such as ethylene, yield of carbon is proportional to the conversion. In the process of coke formation, some ethylene is used in the polymerization reaction and that part of the ethylene is not available for alkylation reaction; and this reduces the conversion.

The activity curves (Figures 23 and 24) are similar to those reported in the literature[20,110,111] for various other reactions. The life time of most of the catalysts studied is 4-5 hours, which is in agreement with that reported by Venuto and Landis[111] in case of REX as catalyst for vapour phase alkylation of benzene with ethanol under similar conditions.

The results discussed above may be summarized as follows :

(a) Progressive exchange of Na^{+} ions with RE^{3+} ions in X and Y type zeolites brings about a reduction in the sorption capacity for nitrogen as well as surface areas. The rates and equilibrium sorption of water, ethanol benzene and ethyl benzene also follow the same order as for nitrogen.

(b) The Dubinin Raduskevich equation for micropore filling is applicable to the above data. The micropore volumes thus evaluated decrease with the increased degree of substitution of rare-earth in both X and Y type zeolites.

(c) The thermal stability of zeolites increases with the increase in the degree of exchange. The Y type zeolites with higher silica alumina ratio are more stable as compared to the X type zeolites. This data is supported by the infrared spectra.

(d) The activity of the rare-earth exchanged zeolites for ethylation of benzene increases with the reduction in sodium content in the zeolite and also depends on the silica alumina ratio in the catalyst. A partial substitution of H^+ for Na^+ in the rare-earth zeolite enhances the catalytic activity.

***

REFERENCES

REFERENCES

(1) W.M. Meier, "Molecular Sieve", Society of Chemical Industry, London, p. 10 (1968).

(2) W.M. Meier and D.H. Olson, Advan. Chem. Series, Molecular Sieve Zeolites - 1, 101, 155 (1971).

(3) R.M. Barrer, F.W. Bultitude and J.W. Sutherland, Trans. Faraday Soc., 53, 1111 (1957).

(4) G. Bergerhoff, H. Koyama and W. Nowacki, "Experimentia", 12, 418 (1956).

(5) J. Turkewich, Catalysis Reviews, 1, 1 (1968).

(6) D.W. Breck, "Zeolite Molecular Sieves, Structure, Chemistry and Use", Pub. Wiley Interscience, New York, (1974).

(7) J.V. Smith, Advan. Chem. Series, "Molecular Sieve Zeolites-I", 101, 171 (1971).

(8) L.V.C. Rees, Annual Report, Progr. Chem., 67A, 191 (1970).

(9) I.D. Mikheikin, Russian Chemical Reviews, 41, 468 (1972).

(10) R. Rabinowitch and W.C. Wood, Trans. Faraday Soc., 32, 947 (1936).

(11) R.M. Barrer, Proc. Roy. Soc., A167, 392 (1938).

(12) R.M. Barrer and A.B. Robins, Trans. Faraday Soc., 49, 929 (1953).

(13) B.P. Bering, M.M. Dubinin, E.G. Zhukovskaya and V.V. Serpinskii, Russ. J. Phy. Chem., 40, 296 (1966).

(14) P.H. Emmett and T.W. Dewitt, J. Am. Chem. Soc., 65, 1253 (1943).

(15) R.M. Barrer and L.V.C. Rees, Trans. Faraday Soc., 50, 852, 989 (1954).

(16) L.V.C. Rees and T. Berry, "Molecular Sieves" Soc. Chem. Industries, London, page 149, (1968).

(17) R.M. Barrer and J.W. Sutherland, Proc. Roy. Soc., A237, 439 (1956).

(18) R.M. Barrer and G.C. Bratt, J. Phy. Chem. Solids, 11, 130, 146, 154 (1959).

(19) R.M. Barrer and R.M. Gibbons, Trans. Faraday Soc., 61, 948 (1965).

(20) R.M. Barrer and W.I. Stuart, Proc. Roy. Soc., A249, 464, 484 (1959).

(21) R.M. Barrer and R.M. Gibbons, Trans. Faraday Soc., 59, 2569, 2875 (1963).

(22) M.M. Dubinin, E.G. Zhukovskaya and K.O. Murdmaa, Bull. Akad. Sci. U.S.S.R., Chem. Ser., 708, 896 (1962).

(23) B.G. Aristov, A.V. Bezus and A.V. Kiselev, Russ. J. Phy. Chem., 41, 1691 (1967).

(24) B.G. Aristov, V. Bosacek and A.V. Kiselev, Trans. Faraday Soc., 63, 2057 (1957).

(25) B.G. Aristov, and A.V. Kiselev, Kolloid Zh., 29, 749 (1967).

(26) J.A. William and H.F. William, J. Catalysis, 14, 118 (1969).

(27) G.T. Kerr, J. Catalysis, 15, 200 (1969).

(28) A.P. Bolten and M.A. Lanewala, J. Catalysis, 18, 154 (1970).

(29) R.M. Barrer and D.A. Langley, J. Chem. Soc., 3804 (1958).

(30) P.B. Venuto and P.S. Landis, Advan. Catal. Relat. Subj., 18, 259 (1968).

(31) H.F. Leach, Annual Reports; Chem. Soc., 68, 195 (1971).

(32) Kh. M. Minachev and Ya. I. Isakov, Advan. Chem. Series, 121, 451 (1973).

(33) V.J. Frilette, P.B. Weise and B.L. Golden, J. Catalysis, 14, 301 (1962).

(34) Brit. Pat. 886,716 (1962).

(35) D.W. Besset and H.W. Habgood, J. Phy. Chem., 64, 769 (1960).

(36) T. Yashima, Y. Ushida, M. Ebisawa and N. Hara, J. Catalysis, 36, 320 (1975).

(37) N.E. Cross, C. Kemball and H.F. Leach, J. Chem. Soc., A21, 3315 (1971).

(38) Z.V. Gryanova, I.V. Metnichenko and K.A. Baskunyan, Kinet. Katal., 13, 141 (1972).

(39) A.M. Rubinshtein, Kh. M. Minachev, A.A. Slinkin, V.I. Garanin and G.A. Ashavskaya, Bull. Akad. Sci. USSR, Chem. Ser., 757 (1968).

(40) V. Penchev, D. Davidova, V. Kanazirev, H. Minachev and Y. Neimark, Advan. Chem. Ser., 121, 461 (1973).

(41) I. Mochida, S. Hayate, A. Kato and T. Seiyama, J. Cat., 15, 314 (1969); ibid, 19, 405 (1970).

(42) P.B. Venuto, Advan. Chem. Ser., 102, 260 (1971).

(43) Japanese Pat. 7401,525 (1974).

(44) Japanese Pat. 2065,632 (1974).

(45) Ya. I. Isakov, Kh. M. Minachev, V.P. Kalinin, Izv. Nauk. SSSR. Ser. Khim., 5, 1138 (1973).

(46) Kh. M. Minachev, Ya. I. Isakov, V.V. Mirzabekov, V.I. Bogomolov, Nefte-Khimiya, 13, (3), 407 (1973).

(47) U.S.A. Pat., 1,468,982 (1973).

(48) Lacko Rafael, Chemla Miloslav, Hala Zadislav, Ropu Uhlie, 14(6), 301 (1972).

(49) U.S. Pat., 3,251,847 (1966).

(50) U.S. Pat., 6,407,674 (1966).

(51) J.A. Rabo, C.L. Angell, V. Schomaker, Proc. 4th Int. Cong. Catal., 2, 96 (1968). (Pub. 1971)

(52) F.W. Kirsch, J.D. Potts, D.S. Barmby, J. Catal., 27(1), 142 (1972).

(53) Yashima Tatsnaki, Ahmad Habib, Yamazaki Kaora, Katsuto Masatoshi, Hara Nobuyoshi, J. Catalysis, 16(3), 273 (1970).

(54) I.M. Kolesnikov, G.M. Panchenkov and V.A. Tret'yakova, Zh. Fiz. Khim., 41(5), 1114 (1967).

(55) P.B. Venuto, P.S. Landis and L.A. Hamilton, Amer. Chem. Soc., Div. Petrol. Chem. 11(1), 91 (1966).

(56) P.B. Venuto, L.A. Hamilton and P.S. Landis, J. Catalysis, 5(3), 84 (1966).

(57) V.I. Vogel, "A Textbook of Qualitative Inorganic Analysis" p.254.

(58) L.G. Joyner, "Scientific and Industrial Glass Blowing and Laboratory Techniques", p. 257, Edited by W.E. Barr and V.J. Anhorn (1949).

(59) F. Paulick and J. Paulick and L. Erdey, Talanta, 13, 1405 (1966).

(60) R.M. Barrer and B.F. Fender, J. Phy. Chem. Solids, 21, 1, 12 (1961).

(61) J.A. Rabo, C.L. Angell, P.H. Kasari and V. Schomaker, Disc. Faraday Soc., 41, 328 (1965).

(62) A.V. Kiselev, Disc. Faraday Soc., 40, 205 (1965).

(63) G.V. Tsitsishvili and T.G. Andronikashvili, "Molecular Sieve Zeolites-II" Advan. Chem. Ser., 102, 220 (1971).

(63A) G.V. Tsitsishvili, Russ. J. Phy. Chem., 46,1723 (1972).

(64) G.R. Landolt and G.T. Kerr, Separation and Purification Methods, 2(2), (1973).

(65) J. Hopper, Ph.D. Thesis, A study of the catalytic Hydro-isomerization Reactions, University Microfilm, Inc. Ann., Arbor Michigen (1969).

(66) H.W. Habgood, Canadian J. Chem., 36, 1384 (1958).

(67) K.I. Skobetskaya, T.R. Bruena and A.M. Rubinshtein, Bull. Akad. Sci. USSR, 33 (1968).

(68) M.M. Dubinin and L.V. Randushkevich, Doklady Akd. Nauk. SSSR, 55, 327 (1947).

(69) D.W. Breck and R.W. Grose, Advan. Chem. Series, 102, 319 (1973).

(70) D.W. Breck, J. Chem. Education, 41, 678 (1964).

(71) D.W. Breck, "Zeolite Molecular Sieves" Pub. John Wiley and Sons, p. 613 (1973).

(72) M.M. Dubinin, E.G. Zhukovskaya, K.O. Murdmma and E.F. Polstyanov, Bull. Akad. Sciences USSR, 2023 (1962).

(73) R.M. Barrer, Advan. Chem. Ser. "Molecular Sieve Zeolites-II" 102, 1 (1971).

(74) R.M. Barrer and D.W. Breck, Trans. Faraday Soc., 49, 1049 (1953).

(75) D.W. Breck, "Zeolite Molecular Sieves", Pub. John Wiley and Sons, p. 49, 63 (1973).

(76) R.K. Sethi and S.L. Chopra, Indian J. Chem., 14A, 94 (1976).

(77) P.B. Venuto and P.S. Landis, Advan. Catal. Relat. Subj., 18, pp.267-271 (1968).

(78) D.W. Breck, "Zeolite Molecular Sieves", Pub. John Wiley and Sons, pp. 674, 684, 688 (1973).

(79) H. Bremer, W. Morke, R. Schödel and F. Vogt, Advan. Chem. Ser., "Molecular Sieve Zeolites", 121, 249 (1973).

(80) H. Bremer, R. Schodel and F. Vogt, Z. Chem., 12, 423 (1972).

(81) B.V. Romanovskii, Russ. J. Phy. Chem., 45, 270 (1970).

(82) G.O. Piloyan and O.S. Novikova, Russ. J. Inorg. Chem., 19, 313 (1967).

(83) A.W. Coats and J.P. Redfern, Nature, 201, 68 (1964).

(84) H.E. Kissinger, Analyst. Chem., 29, 1702 (1957).

(85) I.S. Rassonskaya, "Thermal Analysis" Vol. 2, page 953, Edited by Robert F.

(86) G.O. Piloyan and O.S. Novikova, Inorganic Materials, 2, 1109 (1966).

(87) S.P. Zhadnov, A.V. Kiselev, V.I. Lygin and T.T. Titova, Russ. J. Phy. Chem., 38, 1299 (1964).

(88) A.C. Wright, J.P. Rupert and W.P. Granguist, Amer. Miner., 53, 1293 (1968).

(89) E.M. Flanigen, H. Khatami and H.A. Szymanskii, Advan. Chem. Ser., 101, 201 (1971).

(90) P.B. Venuto, Chem. Tech., 1, 215 (1971).

(91) R.L. Mays and E. Picket, "Molecular Sieves" Soc. Chem. Industries London, p. 112 (1968).

(92) J.A. Rabo, C.L. Angell and V. Schomaker, Proc. 4th Intn. Cong. Catal. (Moscow), 3, 966 (1968).

(93) Y. Morita, H. Takayasu and H. Matsumato, Kogyo Kazaku Zasshi, 73, 2540 (1970).

(94) German Patent 1934,426 (1970).

(95) German Patent 1931,425 (1970).

(96) C.J. Johny, A.J. Chandwadkar, G.V. Potnis, M.U. Pai and S.B. Kulkarni, Ind. J. Technology, 1976 (Communicated).

(97) P.E. Pickert, J.A. Rabo, E. Dempsy, V. Schomaker, Proc. 3rd Intern. Cong. Catal. (Amsterdam), 1, 714 (1965).

(98) J.W. Ward, J. Catalysis, 10, 34 (1968).

(99) J.W. Ward, J. Catalysis, 14, 365 (1969).

(100) J. Turkevich and Y. Ono, Advan. Chem. Ser., "Molecular Sieve Zeolites-II", 102, 315 (1971).

(101) N.E. Cross, C. Kemball, H.F. Leach, Advan. Chem. Ser., "Molecular Sieve Zeolites-II", 102, 389 (1971).

(102) D. Ballivet, P. Pichat, and D. Berthmeuf, "Molecular Sieve Zeolites", Advan. Chem. Ser., 121, 469 (1973).

(103) K.V. Topchieva and E.N. Rosolovskaya, Russ. J. Phy. Chem., 44, 484 (1970).

(104) Y.N. Sidorenko and P.N. Galich, Ukrain Khim. Zhur, 36, 1234 (1970).

(105) Kazuo Tsutsumi and Hiroshi Takahashi, J. Catalysis, 24, 1 (1972).

(106) J.W. Ward, J. Catalysis, 17, 355 (1970).

(107) S.E. Tung and E. Meininch, J. Catal., 10, 175 (1968).

(108) P.B. Venuto and P.S. Landis, Advan. Catal. Relat. Subj., 18, 275 (1968).

(109) M.A. Tanatorov, G.M. Panchenkov, M.E. Levinter, Russ. J. Phy. Chem., 40, 850 (1966).

(110) P.B. Venuto and P.S. Landis, Advan. Catal., Relat. Subj., 18, p. 323 (1968).

(111) J.P. Nolley (Jr.) and J.R. Katzer, "Molecular Sieve Zeolites", Advan. Chem. Ser., 121, 563 (1973).

***

SUMMARY

S U M M A R Y

A series of rare-earth exchanged and a few rare-earth and ammonium exchanged X and Y type zeolites are prepared. The structural properties of these zeolites are examined by X-ray, infra-red, thermal (DTA, TGA) and sorption measurements.

A correlation between effect of degree of exchange and the stability of the framework structure of the zeolites has been studied with the measurement of sorption of nitrogen at 78°K and the vapours of solvents like water, benzene, ethanol and ethyl benzene at 25°C. From the nitrogen adsorption at 78°K; the surface areas are calculated applying Langmuir and BET equations. A progressive reduction in the sorption capacity for nitrogen and surface area is observed in both X and Y type zeolites. Nitrogen adsorption isotherms are also analysed in terms of Harkins-Jura equations. The H.J. plots yield two different straight lines, except for NaX and NaY indicating its inapplicability to the nitrogen adsorption data in the zeolites. The H.J. surface areas calculated, using the slopes of the straight lines for NaX and NaY, were abnormally high as compared to those obtained from BET and Langmuir approach.

The applicability of Dubinin's equation to the sorption of nitrogen in zeolites has been examined and from the Dubinin's plots, void volumes of various zeolites have been evaluated. The void volumes are found to decrease with the increase in the sodium replacement with rare-earth. Differential free energy ($\triangle G^{\circ}$) of adsorption is calculated from the nitrogen adsorption isotherms. The value of $\triangle G^{\circ}$ is found to decrease with the surface coverage and for the same value of $\triangle G^{\circ}$ the amounts sorbed decrease with the increase in the sodium replacement.

The rate as well as equilibrium sorption values for the solvent vapours (water, ethanol, benzene and ethyl benzene) are found to decrease with the increased replacement of sodium ions with rare-earth or rare-earth and hydrogen ions in NaX and NaY zeolites. The degree of sorption is found to be dependent upon the polarity and size of the adsorbate molecule. The sorption capacity for zeolites in higher range of exchange ($>80\%$) is reduced. This is attributed to the occupancy of the relatively less screened S_{II} sites in the supercages.

The diffusion coefficients are calculated from th rate measurements for the adsorption of solvent vapours using the method employed by Barrer. The diffusion coefficients are obtained from the plot of $Q_t - Q_o / Q$, against $/\overline{t}$. The external surface area (A) and

of the zeolite powder have also been determined. The diffusion coefficient of water is found to decrease with progressive exchange; on the other hand the diffusion coefficient increased with the degree of exchange in the case of ethanol, benzene and ethyl benzene as sorbates. The dimension and polarity of sorbate molecules is found to influence the diffusion coefficient.

The thermal stability of the zeolites is estimated from DTA and TGA curves. The temperatures of the minima of the endothermic peak and that of the maxima of the exothermic peak are found to increase with the replacement of sodium ion by rare-earth and hydrogen ions. This indicates an increased thermal stability. The decrease in the loss in weight in the TGA curve is a consequence of a decrease in the sorption capacity. The energy of activation for dehydration of zeolites calculated from DTA, TGA curves by employing three different kinetic equations ranges between 4 to 7 Kcals/mole and is found to be somewhat lower for the zeolite containing hydrogen ions. The order of reaction for the dehydration of zeolites is evaluated from DTA curves by the "shape index" method. The dehydration is found to occur in accordance with the first order kinetics.

The structural changes in the exchanged zeolites are also characterised from infra-red spectral studies.

The intensity of the i.r. bands is found to decrease with degree of exchange in X type zeolites. On the other hand, there are less significant changes in spectra of Y type zeolites as compared to those in X type zeolites, which indicates that Y type zeolites are more stable as compared to the X type zeolites.

X-ray powder photographs ascertain that the crystalline nature of the zeolite is retained on exchange with the rare-earth and hydrogen ions.

The catalytic activity of the rare-earth and hydrogen exchanged X and Y type zeolites, is tested for the vapour phase alkylation of benzene with ethanol. The quantity of ethyl benzene formed in the reaction is taken to be a measure of catalytic activity. The catalytic activity is found to increase with the rare-earth content in the zeolite. The activity is enhanced by the introduction of hydrogen ions in addition to rare-earth ions in the zeolite. The catalytic activity is related to the Brönsted acid centres and to the silica-alumina ratio in the zeolite. In general, Y type zeolites are found to be more active than the corresponding X type catalysts. The fall in the activity after 4-5 hours reaction time is attributed to the formation of higher polymers of ethyl benzene, ethylene which lead to the coke formation. A sharp

fall in the activity is observed in the case of most active catalyst while a gradual decrease extending over a period of several hours is noted in the catalyst sample having low activity.

From the above studies it may be concluded that the sorption and catalytic properties of zeolites depend on the silica alumina ratio (R) and also on the nature and concentration of cations. The type Y zeolite (R = 4.26) is more active and stable as compared to the X type zeolite (R = 2.56). The structural characteristics are evaluated from the X-ray diffraction, i.r., D.T.A., T.G.A. and sorption properties of the zeolites.

***